# Studies on the functions of *Haemaphysalis longicornis* C-type lectin, and its relationship with *Babesia* parasites

（フタトゲチマダニ由来 C 型レクチンの機能と
バベシア原虫との関連性に関する研究）

**Doctoral Dissertation**

**The United Graduate School of Veterinary Science,
Yamaguchi University**

**Hiroki MAEDA**

**March 2017**

# TABLE OF CONTENTS

# LIST OF TABLES AND FIGURES

**CHAPTER 1**



**CHAPTER 2**

**CHAPTER 3**



**CHAPTER 4**

# ABBREVIATIONS

AMPs: antimicrobial peptides
cDNA: complementary DNA
Clec: C-type lectin
COMP: Cartilage oligomeric matrix protein
CRD: carbohydrate recognition domain
DAB: 3,3' diaminobenzidine
DPE: days post engorgement
dsRNA: double-stranded RNA
EST: expressed sequenced tag(s)
FBS: fetal bovine serum
His: histidine
*HlCLec*: *Haemaphysalis longicornis* C-type lectin gene
HlCLec: *Haemaphysalis longicornis* C-type lectin protein
IFAT: indirect immunofluorescent antibody test
IPTG: isopropyl β-D-1-thiogalactopyranoside
LB: Luria-bertani
*Luc*: firefly luciferase gene
mRNA: messenger RNA
ORF: open reading frame
PAMPs: pathogen-associated molecular patterns
PBS: phosphate-buffered saline
qPCR: quantitative polymerase chain reaction
RBC: red blood cells
RNAi: RNA interference
RT-PCR: reverse transcription polymerase chain reaction
PRR: pattern recognition receptor
SDS-PAGE: sodium dodecyl sulfate-polyacrylamido gel electrophoresis
SFTS: severe fever with thrombocytopenia syndrome
TBS: tris-buffered saline
TLR: toll-like receptors
TSB: Bacto™ Tryptic Soy Broth medium
WBC: white blood cells

# GENERAL INTRODUCTION

## Ticks as vectors: focused on their innate immunity

Ticks are notorious hematophagous ectoparasites of almost all terrestrial vertebrates and well known as a unique vector of various deadly diseases, such as Lyme borreliosis, tularemia, anaplasmosis, babesiosis, theileriosis, tick-borne encephalitis, and severe fever with thrombocytopenia syndrome (SFTS) [1, 2]. About 900 tick species, including approximately 700 ixodids and 200 argasids, are distributed throughout the world [3, 4]. Recent analysis of the tick microbiome indicates that ticks harbor a wide variety of microorganisms [5]. Pathogens, including bacteria, protozoa, and viruses, are taken up with the blood meal and exposed to a potentially hostile environment in the tick's midgut before they invade the gut cells. It is assumed that the tick-pathogen interaction in relation to the adaptation and proliferation of the pathogens in ticks and their successful transmission to the vertebrate hosts is maintained by molecular mechanisms [6, 7].

Babesiosis is caused by intraerythrocytic apicomplexan parasites which belong to the genus *Babesia* and is mainly transmitted by tick vectors to a variety of vertebrate hosts, including wild and domestic animals and also humans [8, 9]. *Babesia* species undergo a complex developmental cycle in the vertebrate host and tick, somewhat analogous to that of malaria parasites and their mosquito vector. With the worldwide distribution of ixodid ticks, babesiosis is the second most common blood-borne disease

of mammals. The major tick vectors of *Babesia* globally are the *Rhipicephalus* and *Haemaphysalis* species [10]. The ixodid tick *H. longicornis*, one of the most important tick species in Asia and Australia, is a natural vector of the protozoa that causes babesiosis in humans and domestic animals [11]. It has been shown that the bioactive molecules such as longicin and longipain from *H. longicornis* critically regulates the transmission of *Babesia* parasites in the tick [12, 13].

In invertebrates, the innate immune system is the first line of host defense for sensing invading pathogens by recognition of their specific structural components (pathogen-associated molecular patterns: PAMPs) through pattern recognition receptors (PRRs) [14, 15]. The outer exoskeleton, the midgut epithelium, and the lining of the trachea are considered as the first defense barriers. However, these barriers cannot prevent the invasion of adapted pathogens, and then, they will become as the vector. After allowing the invasion of pathogens, they are exposed to humoral and cellular responses [10, 11].

Here, I simply overview the main events of innate immunity of invertebrates:

Humoral defenses in invertebrates

1. Antimicrobial peptides (AMPs)

Antimicrobial peptides, a group of low molecular weight natural compounds that exhibit antimicrobial activity consists of a large family. The peptides are mainly synthesized in the fat body. To date, over hundreds of AMPs are identified and characterized in invertebrates [16, 17].

2. Lectin (Agglutinin)

Lectins (or sometimes terms as agglutinin) exist in all living organism and consist of some large families which have the ability to bind to specific carbohydrates expressed on different cell surfaces. Thus, they play important roles in the reaction of non-self recognition [18].

3. Prophenoloxidase (Pro-PO) cascade (melanization system)

Several groups of invertebrates are known to synthesized melanized capsules including fungi or bacteria. The melanin with toxic quinone substances is synthesized by phenoloxidase made from its precursor Pro-PO exists in their

hemolymph. It is also known that this reaction participate in the wound healing process in the damaged cells. [19, 20].

Cellular events in invertebrates (hemocyte-mediated immune responses)

1. Phagocytosis

Hemocytes, circulating blood cells, are primary mediators of innate immunity of invertebrates, which will become active for pathogen trapping and elimination by digestion [21, 22].

2. Encapsulation

The invaders are encapsulated by multi-cellular sheaths, which consists by plasmatocytes, they are participated after the degranulation of granulocytes. Granulocytes are similar to mammalian neutrophil granulocytes and can also be numerous. Plasmatocytes are morphologically close to mammalian monocytes but are not numerous. Following the encapsulation, typical melanization will occur [21, 22].

3. Nodulation

In face of the large number of pathogens, they are entrapped in the materials like strings released by granulocytes, and melanization occurs externally. After

then, plasmatocytes adhere and form multi-cellular sheaths containing necrotic core of melanized pathogens [21, 22].

In innate immunity of ticks, there are also similar as mentioned above, however, ticks lacks Pro-PO activation system leading to melenization [23, 24]. In encapsulation and nodulation, there are reports only about *Dermacentor* species of ticks [25, 26], therefore, these responses might be species specific. Taken above, generally in tick's innate immunity, it is considered that phagocytosis as cellular responses, and AMPs and lectins as humoral responses are mainly important. To date, lots of AMPs are identified and characterized in ticks, however, there are fewer reports on tick lectin, especially, C-type lectin (CLec) than those of AMPs [27, 28]. Thus, I would like to identify a novel CLec from ticks and clarify their functions.

Currently, some PRRs including Toll-like receptor (TLR) have been already identified and classified [29, 30]. CLec is also known as one of the PRRs playing important roles in non-self clearance of pathogens [31, 32]. CLec consists a large family containing at least one carbohydrate recognition domain (CRD), which share a common structure, such as the EPN motif and QPD motif for the carbohydrate recognition. Although CLec also recognize non-carbohydrate matters, the mechanisms are not fully

understood [33]. Due to the fact that lectins have the ability to bind carbohydrate and promote the agglutination of different cells, such as invading pathogens, it is reasonable to assume that they have a potential role in invertebrate non-self recognition reactions. From above, I considered that the lectin of ticks might have important roles for the defense mechanism against invading pathogens.

In this dissertation, I focused on the CLec in ticks and their roles in the infection of pathogens.

## Research Objectives

With following objectives, the studies on CLec of *H. longicornis* ticks (HlCLec) and its relationship with *B. ovata* are described in this dissertation.

AIM 1. To identify and characterize of HlCLec

AIM 2. To clarify the migration of *Babesia* parasites in the ticks

AIM 3. To clarify the development of *Babesia* paraites in the ticks

AIM 4. To evaluate the relationship with HlCLec and *Babesia* parasites

# CHAPTER 1

## Identification and characterization of a novel C-type lectin from *Haemaphysalis longicornis*

**This work has been published as:**

Maeda, H., Miyata, T., Kusakisako, K., Galay, R.L., Talactac, M.R., Umemiya-Shirafuji, R., Mochizuki, M., Fujisaki, K. & Tanaka, T. (2016). A novel C-type lectin with triple carbohydrate recognition domains has critical roles for the hard tick *Haemaphysalis longicornis* against Gram-negative bacteria. *Dev. Comp. Immunol.*, ***57***, 38-47.

## 1.1 Introduction

Ticks are capable of transmitting a wide variety of pathogens, and are ranked second only to mosquitoes as vectors. Even though their vector competence is considered closely involved to their immune system, the detailed knowledge of tick innate immunity is insufficient [7, 23, 24]. The lectin of ticks have not received the same attention level as those of other species [27]. Papers on tick lectins that have been published were very few, and more research data are needed to complete our knowledge for the role of lectin in the immune system of ticks. CLec is also considered to have an important role in tick innate immunity; however, only a few number of CLec were identified in ticks. In *Ixodes scapularis* genome project, some kinds of CLecs were found, but their function remains unknown [34]. In contrast, many CLec were identified and functionally analysed in various invertebrates [35–37]. In the blood-sucking mosquitoes, CLec has key role in anti-*Plasmodium* and antibacterial defense mechanisms [38].

Here, I studied a novel CLec has been identified and characterized from the hard tick, *H. longicornis* (HlCLec).

## 1.2 Materials and Methods

### *1.2.1 Ticks and Animals*

The parthenogenetic Okayama strain of *H. longicornis* has been maintained by blood feeding on ears of 2 month-old female Japanese white rabbits (Kyudo, Kumamoto, Japan) [39] in the Laboratory of Infectious Diseases, Joint Faculty of Veterinary Medicine, Kagoshima University. Rabbits and 4 weeks-old female ddY mice (Kyudo) were cared for in accordance with the guidelines approved by Animal Care and Use Committee of Kagoshima University (Approval no. VM13007). They were maintained under a regulated condition throughout experiments.

### *1.2.2 Identification and characterization of cDNA encoding the C-type lectin*

The putative C-type lectin was identified using expressed sequence tags (EST) database constructed from the cDNA library of ovary. pGCAP1 plasmid containing HlCLec gene-encoding insert was extracted using Qiagen® Plasmid Mini Kit (Qiagen, Hilden, Germany). The insert was sequenced by Big dye® Terminator v3.1 Cycle Sequencing Kit (Applied Biosystems, CA, USA) using Applied Biosystems® 3500 XL Genetic analyzer (Applied Biosystems). The deduced amino acid translation of the

HlCLec sequence was determined by GENETYX version 7.0 software (GENETYX, Tokyo, Japan). To search homologous genes from GenBank (http://www.ncbi.nlm.nih.gov/genbank), BLAST server (http://blast.ncbi.nlm.nih.gov/Blast.cgi) was used. The domain structure was determined by SMART program (http://smart.embl-heidelberg.de/). The theoretical molecular weight and isoelectric point were computed using ProtParam tool (http://web.expasy.org/protparam/). Putative signal peptide cleavage sites and N-linked glycosylation sites were determined by SignalP 4.1 server (http://www.cbs.dtu.dk/services/SignalP/) and NetNGlyc 1.0 server (http://www.cbs.dtu.dk/services/NetNGlyc/), respectively.

### *1.2.3 Expression and purification of recombinant HlCLec and its individual CRDs*

The sequences of recombinant HlCLec were designed to contain all CRDs (39-452) for mature HlCLec, and CRD2 and CRD3 (193-535) for partial HlCLec, and for the individual CRD namely CRD1 (39-167), CRD2 (191-312), or CRD3 (333-452) (Fig. 1.6, 1.7). They were amplified using specific primer sets by PCR (Table 1.1). After purifying the PCR products using a GENECLEAN® II KIT (MP Biomedical, Solon, OH, USA), they were subcloned into the frame of pRSET B using a *Bam*H I and *Eco*R I recognition sites for partial HlCLec, and *Nco* I and *Hin*d III recognition sites for others. Recombinant

plasmids were transformed into an *E. coli* BL21(DE3) strain and expressed by induction with 1 mM isopropyl-β-D(-)-thiogalactopyranoside (IPTG) at 37°C for 4 h. Expressed recombinant proteins were purified by a His-trap FF column (GE Healthcare, Buckinghamshire, UK) using a Bio Logic Duo Flow Base System (BIO-RAD, Tokyo, Japan) from insoluble fraction under denaturing condition. The purified recombinant proteins were dialyzed against Tris-buffered saline (TBS) solution. The purity of the recombinant proteins were checked by SDS-PAGE. The concentrations of recombinant proteins were determined by a Micro BCA™ protein assay kit (Thermo Fisher Scientific, Rockford, IL, USA), and stored at -30°C until use.

### *1.2.4 Production of an anti-serum against partial HlCLec*

To prepare mouse anti-HlCLec sera, 100 μg of recombinant partial HlCLec completely mixed with Freund's complete adjuvant (Sigma-Aldrich, St. Louis, MO, USA) was intraperitoneally injected into mice. After 2 weeks, these mice were injected with 100 μg of recombinant partial HlCLec mixed with Freund's incomplete adjuvant (Sigma-Aldrich) twice at 2-week intervals to boost the generation of antibodies. Blood was collected 2 weeks after the third immunization to obtain the specific antisera for HlCLec.

### *1.2.5 RNA extraction and cDNA synthesis*

To extract total RNA, whole ticks were homogenized using an Automill (Tokken, Chiba, Japan), while dissected organs were disrupted using a pellet pestle motor (Sigma-Aldrich), and then TRI® reagent (Sigma-Aldrich) was added. The extracted RNA was purified with a Turbo DNA-*free*™ Kit (Applied Biosystems). cDNA synthesis was performed with ReverTra Ace-α-® (TOYOBO, Osaka, Japan) using 1 μg of total RNA according to the manufacturer's protocol.

### *1.2.6 Expression analysis of the HlCLec mRNA*

The expression analysis of the *HlCLec* mRNA was performed by quantitative PCR (qPCR) using THUNDERBIRD™ SYBR® qPCR Mix (TOYOBO) with a 7300 qPCR system (Applied Biosystems). Gene-specific primers were designed to target the *HlCLec* and the control genes, as shown in Table 1.1. Standard curves were made from eight-fold serial dilutions of cDNA of adult ticks fed for 3 days. The PCR cycle profile was as follows: 95°C for 10 min, 40 cycles of a denaturation step at 95°C for 15 sec, and an annealing/extension step at 60°C for 60 sec. The data was analyzed with 7300 system SDS software (Applied Biosystems). At the first step of qPCR, *actin*, *tubulin*, *P0*, and *L23* genes were evaluated for standardization and *actin* was selected for tick reference.

### *1.2.7 Indirect immunofluorescent antibody test (IFAT)*

Three days-partially fed ticks were dissected under the stereo microscopy (SZX10, Olympus, Tokyo, Japan) for collecting tick organs. Dissected organs were separately fixed in 4% paraformaldehyde phosphate buffer solution (pH 7.4) including 0.1% glutaralaldehyde at 4°C overnight. After washing with a sucrose series, organs were embedded in Tissue-Tec® O.C.T Compound (Sakura Finetek, Torrance, CA, USA). 10 μm of frozen sections were cut using a cryostat (Leica CM 1850, Leica Microsystems, Wetzlar, Germany), placed on the slide glasses. The slides were blocked with 5% skim milk in phosphate buffered saline (PBS, pH 7.4) at 37°C for 1 h, and then incubated with 1:100 dilution in blocking solution of anti-HlCLec mouse serum at 37°C for 1 h. For the negative control, normal mouse serum was used. After washing three times in PBS, the slides were incubated at 37°C for 1 h with Alexa Fluor® 594-labeled goat anti-mouse IgG (Invitrogen, Carlsbad, CA, USA) with 1:1000 dilution in blocking solution. After removing of unbounded antibody by washing three times with PBS, samples were mounted with DAPI (VECTASHIELD®; Vector Laboratories, Burlingame, CA, USA), then covered with a cover glass. The images were recorded using a confocal laser scanning microscopy (LSM700, Carl Zeiss, Jena, Germany).

### *1.2.8 RNA interference (RNAi)*

Approximately of 564 bp fragments of *dsHlCLec* was synthesized by specific primer sets (Table 1.1) using the T7 RiboMax$^{TM}$ Express RNAi kit (Promega, Madison, WI, USA) according to the manufacturer's instructions. The firefly luciferase (Luc) gene was used for control. Two microgram of *dsHlCLec* or *dsLuc* was injected into 35 unfed female adult ticks in the experimental and control groups, through the fourth coxae into the hemocoel. Injected ticks were incubated at 25°C for 24 h and fed on the same rabbit with two groups on different ears. Three days after attachment, three ticks were detached for the confirmation of the gene silencing by RT-PCR using the specific primer sets (Table 1.1). The remaining ticks were allowed to feed until engorgement, and the body weight after engorgement and oviposition were monitored.

### *1.2.9 Bacterial binding assay*

Direct binding of recombinant proteins to bacteria was conducted as described previously with a slight modification [40, 41]. *E. coli* (ATCC 25922 strain) and *Staphylococcus aureus* (ATCC 29213 strain) were used in this study. Briefly, overnight cultures of *E. coli* and *S. aureus* in LB broth were centrifuged and cells were washed 2 times with TBS. 200 µl of recombinant proteins (10 µg/ml) were incubated with 500 µl

of bacterial suspension ($OD_{600}$=1.0). After gently rotating at room temperature for 30 min, samples were centrifuged at 6,000 g at 4°C for 5 min. The bacterial pellet were washed 5 times with TBS, and then, bacterial pellets were eluted by 7% SDS and the lysates were applied on 15% SDS-PAGE for western blot analysis. After transferring samples onto a polyvinylidene difluoride membrane (Immobion-P; Millipore, MA, USA), the membrane was blocked with 5% skim milk in PBS and incubated with anti-His antibody (GE healthcare, 1:3000 dilution) followed by incubation with horseradish peroxidase (HRP)-conjugated goat anti-mouse IgG (GE healthcare, 1:5000 dilution). Antibody bindings were visualized using 3,3' diaminobenzidine (DAB). Cartilage oligomeric matrix protein (COMP) was used as a His-tagged control [42, 43]. This analysis was also performed in the presence of 10 mM $CaCl_2$ to know the effect of $Ca^{2+}$.

### *1.2.10 Bacterial growth assay*

Bacterial growth assay was performed with a slight modification as described previously [44]. Briefly, pre-cultured *E. coli* and *S. aureus* in the Bacto™ Tryptic Soy Broth medium (TSB) were diluted to attain $OD_{600}$ of approximately 0.05. Then, 90 µl of bacterial-aliquots were incubated with 10 µl of recombinant proteins at the concentration of 1 mg/ml. Bacterial growth was monitored by measuring absorbance $OD_{600}$ at hourly

intervals to 6 h, 12 h and 24 h. TBS was used for a negative control.

### *1.2.11 Tick survival assay against bacteria*

Two microgram of *dsLuc* or *dsHlCLec* was injected to 25 unfed female adult ticks of respective group. The gene silenced ticks were allowed to feed on the rabbit for 3 days. Three days partially fed ticks were detached, and *E. coli* or *S. aureus* ($2\times10^6$/ticks) was injected. Confirmation of gene silencing was performed using 3 ticks from each groups by RT-PCR. Injected ticks were stored at 25°C incubator. The survival rate was monitored every 24 h. The statistical analysis of log-rank test was performed by GraphPad Prism version 3.0 software (GraphPad Software, San Diego, CA, USA).

### *1.2.12* Statistical analysis

All experiments were conducted in two or three separate trials. Data were statistically analyzed and $P < 0.05$ was considered statistically significant. Log-rank test was used for static of survival curve. Another experiments were analyzed by Mann-Whitney *U* test.

## 1.3 Results

### *1.3.1 Identification and characterization of HlCLec*

The cDNA encoding C-type lectin (HlCLec; Accession no. LC029912) was isolated from EST clones from the ovary cDNA library of *H. longicornis*. The *HlCLec* ORF consists of 1608 bp encoding 535 amino acids (Fig. 1.1). The predicted molecular mass of HlCLec is 60.2 kDa, and the theoretical isoelectric point (p*I*) is 5.7. A putative signal peptide cleavage site was identified between residues 17 (A) and 18 (R), and a conserved transmembrane region at positions 471-493. HlCLec has three CRDs from positions 41 to 165 (CRD1), 187 to 309 (CRD2), and 325 to 449 (CRD3) (Fig. 1.1). To compare the similarity of each CRD with other invertebrate's CRDs, the sequences were aligned. In each CRD, conserved motifs of $Ca^{2+}$ binding site 2 with slight mutation were found (Fig. 1.1, 1.2: QPR; 130-132, QPS; 274-276, and EPS; 417-419). N-linked glycosylation sites (asparagine) were determined at positions 58, 362, and 397. A polyadenylation consensus signal sequence (AATAAA) was identified upstream of the poly A tail (Fig. 1.1). Comparison of each CRD of HlCLec with one another showed varying results, wherein CRD1 has at least 28% homology with CRD2 and CRD3 while CRD2 has 24% homology with CRD3 (Table 1.2). On the other hand, the homology of

CRDs of HlCLec with CRDs from other species CLec was less than 30% (Table 1.3), however, highly conserved cysteine residues involved in the formation of the CRD internal disulfide bridges were confirmed as shown in Fig. 1.2.

### *1.3.2 Transcription profiles of HlCLec mRNA*

The mRNA level of *HlCLec* in whole adults and each organ during blood feeding and in different developmental stages (egg, larval, nymphal, and adult stages) were examined using qPCR. *HlCLec* was significantly up-regulated in the whole adult ticks (Fig. 1.3A). In developmental stages, the expression level of *HlCLec* was extremely up-regulated after blood feeding in the adult stages and seems decreased until nymphal stages of next generation (Fig. 1.3B). In organs, the highest expression level was detected around the end of blood feeding in the midgut and ovary, respectively (Fig. 1.3C). Other organs showed low transcription level of *HlCLec* and only in hemocytes appeared gradually up-regulation during blood feeding (Fig. 1.3C).

### *1.3.3 Localization of HlCLec in the midgut and ovary*

Because of the high expression of *HlCLec* mRNA in the midgut and ovary, the localization of HlCLec in these organs were confirmed by IFAT. In the midgut, the

positive fluorescence of HlCLec was found in the cell membrane and basal lamina of digestive cells. (Fig. 1.4A). In the ovary, HlCLec was also detected in the cell membrane and basal lamina of oocytes and oviduct cells (Fig. 1.4B).

### *1.3.4 Gene silencing effect of HlCLec*

Gene silencing using RNAi technique was performed to clarify the functions of *HlCLec*. Gene silencing level was confirmed by qPCR, which showed that the expression level of *HlCLec* was significantly decreased (Fig. 1.5). Knockdown of *HlCLec* caused significant effects on ticks' engorged body weight, mortality, and hatching rate of larvae, but there were no significant differences in the oviposition (number of eggs and egg weight), and feeding period compared to control ticks injected with *Luc* dsRNA (Table 1.4).

### *1.3.5 Expression of recombinant HlCLec and its individual CRDs*

Sequences encoding mature HlCLec and individual CRDs were subcloned into a pRSET B vector (Fig. 1.6A). Histidine-tagged recombinant fusion proteins were expressed using *E. coli* and purified. The expression and purification of recombinant proteins and were confirmed by SDS-PAGE analysis (Fig. 1.6C). The recombinant

proteins showed the predicted molecular mass as approximately 50 kDa for mature HlCLec, 17.9 kDa for CRD1, 16.4 kDa for CRD2, and 17 kDa for CRD3 (Fig. 1.6B, C). The specificity of the antisera was also determined by Western blot analysis (Fig. 1.8).

### *1.3.6 Impact of recombinant mature HlCLec and individual CRDs on bacteria*

In the bacterial binding assay, recombinant mature HlCLec and individual CRDs have been found to bind both *E. coli* and *S. aureus* (Fig. 1.9, 1.10). Furthermore, this binding ability was unaffected by the presence of $Ca^{2+}$. Fig 1.9 showed more strong bands when using *E. coli* than *S. aureus*. However, there were no growth inhibitory activity on *E. coli* and *S. aureus* (Fig. 1.11).

### *1.3.7 Gene silencing of HlCLec and tick survival after bacterial infection*

To determine *in vivo* functions of HlCLec, *HlCLec* was knockdowned by injecting dsRNA, and the survival rate of *HlCLec* knockdowned-ticks was determined after injection of live *E. coli* and *S. aureus*. The survival rate of ticks was significantly lower after *E. coli* injection in the *HlCLec*-RNAi groups when compared to *Luc*-RNAi control group (Fig. 1.12A). However, the survival rate of *HlCLec*-RNAi group after injection of *S. aureus* did not show significant difference to the control group (Fig. 1.12B).

## 1.4 Discussion

In this study, I identified a novel CLec from hard tick *H. longicornis*. Interestingly, HlCLec has conserved three different CRDs (Fig. 1.1). Although HlCLec showed low similarity to mannose receptors of some species such as the worm *Saccoglossus kowalevskii,* the rat *Heterocephalus glaber*, the oyster *Crassostrea gigas* and so on. Because of the tandem CRDs, putative homologous gene was not found by BLAST analysis. In recent years, many CLec are identified and well-characterized in invertebrates. Interestingly enough, many invertebrate CLec possess tandem CRDs, such as lipopolysaccharide (LPS)-binding protein and multiple saccharide-binding protein from the silkworm *Bombyx mori* [35, 45], CLec from the prawn *Macrobrachium rosenbergii* [40], and CLec from the scallops *Chlamys farreri* [37] and *Argopecten irradians* [46]. Similar to their CRDs, conserved motifs of $Ca^{2+}$-binding site 2 with slight mutation were identified in *HlCLec* each CRDs (Fig. 1.2). This may explain why there was no difference in the result of bacterial binding assay in the presence of $Ca^{2+}$. There were three different carbohydrate-binding motifs in CRDs, suggesting that HlCLec might have a broader recognition capacity to pathogens. CLecs exist as both oligomers and monomers. CLecs belonging to collectin family is known to occur as trimers and the

CRDs are at the top of the trimer and can be functional to enhance interactions with carbohydrate ligands [47, 48]. It might be considered HlCLec contains multi-CRDs to enhance interaction with carbohydrate ligands than form the trimer. Compared with the well-studied vertebrate CLec, little is known about the multidomain lectins in invertebrates because of lack of homology [33]. Thus, further research is needed to classify these molecules and predict their function as well as the evolutionary history.

*HlCLec* mRNA expression was up-regulated during blood feeding, and is highest in the midgut and ovary (Fig. 1.3A, C). In developmental stages, *HlCLec* mRNA expression is greatly elevated in the adult stage after taking blood meal (Fig. 1.3B). These indicate that HlCLec has an important role during blood feeding in the adult stage. During blood feeding, many non-self object enters the tick midgut, considered to be the first major barrier of tick's innate immunity. After dissemination of pathogens into the hemolymph, this can lead to transovarial transmission [49]. Hence, in the engorged female adult ticks, midgut and ovary were considered as the most important organs. HlCLec might protect these organs by recognizing invaders. IFAT experiments showed the localization of HlCLec in the midgut and ovary, and it appeared to be HlCLec exists in the cell membrane and basal lamina of these organs (Fig. 1.4). This result supports the predicted conserved transmembrane structure of HlCLec.

To clarify the HlCLec function in tick physiology, gene silencing experiment was conducted. Significant effects after gene silencing were observed on ticks' engorged body weight, mortality after engorgement, and hatching rate of larvae (Table 1.4). These effects are probably caused by decreased uptake of necessary substances for their metabolism. Some CLec are known as receptor for capture and uptake of foreign substances [50]. Taken together, HlCLec has important roles in the survival and blood feeding of ticks.

To elucidate the possible function of HlCLec in the tick innate immunity, three experiments using Gram-negative or Gram-positive bacteria were carried out. Recombinant proteins of mature HlCLec and individual CRDs were expressed using *E. coli* (Fig. 1.6), and the function of each domains were examined. From the result of bacterial binding assay, HlCLec exhibits binding ability to both *E. coli*, a Gram-negative bacterium, and *S. aureus,* a Gram-positive bacterium. The binding ability seems stronger to *E. coli* than *S. aureus* (Fig. 1.9). This difference in the binding ability may be related to the differences in bacterial cell wall structure. The bacterial cell wall composition of Gram-negative and Gram-positive bacteria is different, such that the peptidoglycan of Gram-positive bacteria contains lipoteichoic acid and is consequently thicker than the peptidoglycan of Gram-negative bacteria that contains lipopolysaccharide (LPS) [51–53].

CLecs might not act as PRRs, but can also mediate direct microbial killing [54, 55]. However, these CRDs have no direct growth inhibiting activity against the tested bacteria (Fig. 1.11). Thus, they might rather act as classical PRRs for bacterial recognition and activate immune-signal pathways. Furthermore, bacterial challenge after *HlCLec* silencing resulted to significant decrease of tick survival rate when *E. coli* was injected, but not when *S. aureus* was injected (Fig. 1.12). LPS is a well-known PAMP of Gram-negative bacteria. To date, many reports showed the interaction of CLecs with LPS [35, 45]. These results strongly suggest the key role of HlCLec as PRRs in the tick innate immunity against Gram-negative bacterial infection. Some CLecs were known to have important roles in hemocytes-mediated innate immunity in invertebrate [56, 57]. Despite the very low gene expression level of *HlCLec* in hemocytes, the expression was up regulated during blood feeding (Fig. 1.3C). HlCLec might be involved with the phagocytic function of hemocytes. However, the precise defense mechanisms against bacterial infection still remains unknown, requiring further studies. The studies on shrimp lectins were relatively well-investigated and Wang and Wang [36] reviewed their functional diversity and variable mechanisms of anti-bacterial immunity. Therefore, there are high possibilities that CLecs in *H. longicornis* possess various functions.

In summary of this Chapter, a novel CLec with triple CRDs was identified from

*H. longicornis*. *HlCLec* was drastically up-regulated during the blood feeding especially in the midgut and ovary. All recombinant CRDs showed binding ability to both *E. coli* and *S. aureus* with no direct-killing. However, only *E. coli* injection after *HlCLec* knockdown caused significant effect on the tick survival rate. Taken together, these results suggest the important role of HlCLec as PRRs for recognition of Gram-negative bacteria in the innate immunity of *H. longicornis*. Further understanding of CLecs of *H. longicornis* might supply information about tick innate immunity and lead to the idea of novel tick and tick-borne pathogens control strategies.

## Tables and Figures in CHAPTER 1

**Table 1.1** Gene specific primers used in Chapter 1

| Primers | Sequence (5' →3') |
|---|---|
| mature HlCLec F-*Nco* I | CATGCCATGGAGGGATACTGCCCCGACAATTGG |
| mature HlCLec R-*Hin*d III | CCCAAGCTTTCATTTTTCCACGGCGCATATG |
| CRD1 F-*Nco* I | CATGCCATGGAGGGATACTGCCCCGACAATTGG |
| CRD1 R-*Hin*d III | CCCAAGCTTTCACCTCTTTTGGCAAACGTGC |
| CRD2 F-*Nco* I | CATGCCATGGGGTCGTTCGAGTACCGGTCTTCG |
| CRD2 R-*Hin*d III | CCCAAGCTTTCAGGTGTTAAACTCGCAAAGG |
| CRD3 F-*Nco* I | CATGCCATGGGGATTGACGTGGGAACTCCTTACTGC |
| CRD3 R-*Hin*d III | CCCAAGCTTTCATTTTTCCACGGCGCATATG |
| partial HlCLec F-*Bam*H I | CGGGATCCGAGTACCGGTCTTCGTGC |
| partial HlCLec R-*Eco*R I | CGGAATTCTCACTCAACGATAGCACT |
| HlCLec RT-F | TATTCTGGACAGGCCTCCAC |
| HlCLec RT-R | ACGAGCCCAATCCATAACTG |
| HlCLec qPCR-F | TGGCTGGAAACGGAACG |
| HlCLec qPCR-R | CATCTGGTCGTTGGAGTGG |
| HlCLec T7-F | ATACTGCCCCGACAATTGGG |
| HlCLec T7-R | GCGTCTCGGATAGACACCAG |
| HlCLec RNAi-F | TAATACGACTCACTATAGGATACTGCCCCGACAATTGGG |
| HlCLec RNAi-R | TAATACGACTCACTATAGGGCGTCTCGGATAGACACCAG |
| Actin RT-F | CCAACAGGGAGAAGATGACG |
| Actin RT-R | ACAGGTCCTTACGGATGTCC |
| Actin qPCR-F | ATCCTGCGTCTCGACTTGG |
| Actin qPCR-R | GCCGTGGTGGTGAAAGAGTAG |
| Tubulin qPCR-F | TTCAGGGGCCGTATGAGTAT |
| Tubulin qPCR-R | TGTTGCAGACATCTTGAGGC |
| P0 qPCR-F | CTCCATTGTCAACGGTCTCA |
| P0 qPCR-R | TCAGCCTCCTTGAAGGTGAT |
| L23 qPCR-F | CACACTCGTGTTCATCGTCC |
| L23 qPCR-R | ATGAGTGTGTTCACGTTGGC |

Under line shows the T7 RNA polymerase promoter sequence

**Table 1.2** Homology of CRDs of HlCLec with each other

| | HlCLec-CRD1 | HlCLec-CRD2 | HlCLec-CRD3 |
|---|---|---|---|
| HlCLec-CRD1 | | 28 | 30 |
| HlCLec-CRD2 | | | 24 |
| HlCLec-CRD3 | | | |

**Table 1.3** Homology of CRDs of HlCLec with CRDs from other species CLec

| | Is-CRD | Cq-CRD | Dm-CRD | Bm-CRD1 | Bm-CRD2 | Fc-CRD1 | Fc-CRD2 |
|---|---|---|---|---|---|---|---|
| HlCLec-CRD1 | 28 | 29 | 21 | 28 | 24 | 25 | 24 |
| HlCLec-CRD2 | 24 | 30 | 29 | 25 | 27 | 28 | 25 |
| HlCLec-CRD3 | 25 | 30 | 23 | 29 | 24 | 23 | 27 |

**Table 1.4** Gene silencing effects of *HlCLec*

| | Number of ticks | Engorged body weight (mg) | Number of eggs |
|---|---|---|---|
| *dsLuc* | 30 | 267.6±55.8 | 680.5±365 |
| *dsHlCLec* | 30 | 221.5±61.6*** | 572.3±332.5 |

| | Egg weight (mg) | Hatching rate (%) | Mortality after engorgement (%) |
|---|---|---|---|
| *dsLuc* | 114.5±47.7 | 89.6 | 0 |
| *dsHlCLec* | 92.2±45.3 | 66.7* | 25.9*** |

*$P$<0.05, ***$P$<0.01, significantly different by Mann-Whitny $U$ test.

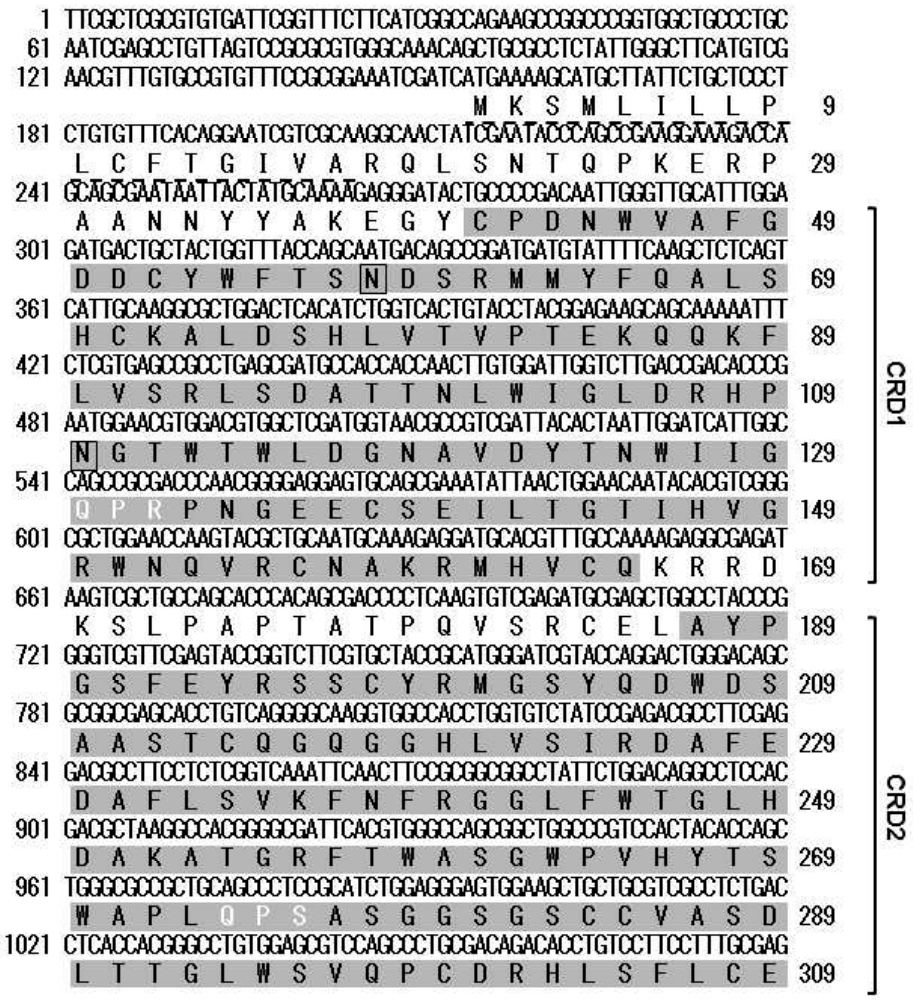


**Fig. 1.1** cDNA and deduced amino acid sequences of HlCLec from *H. longicornis*. The dashed-lined amino acids in the N-terminal show the signal peptide. Putative glycosylated asparagines are boxed. Three CRDs are presented as gray-shaded letters. The conserved $Ca^{2+}$-binding site 2 motifs are shown in white letters. The underlined amino acids in the C-terminal show the transmembrane region. The putative polyadenylation signal after the stop codon has been underlined.

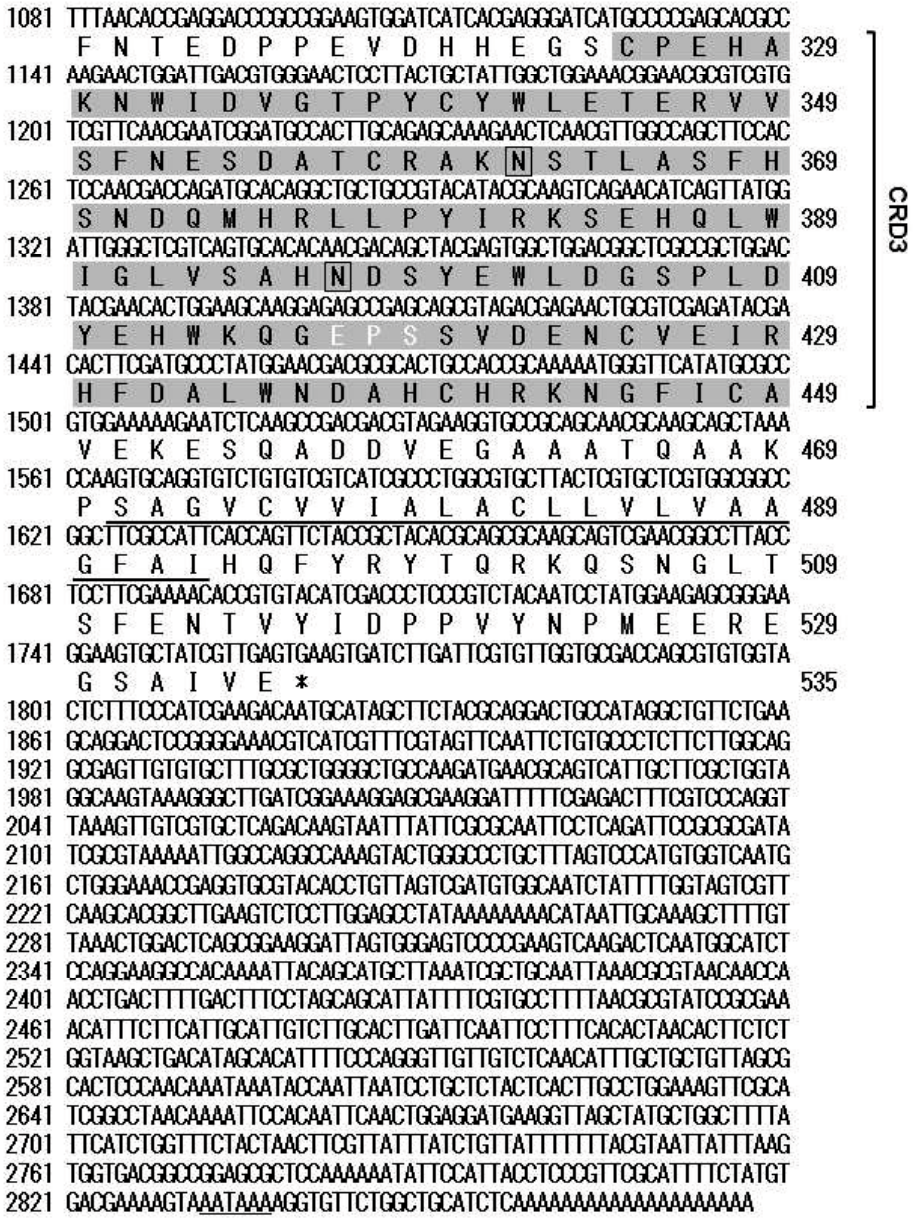


**Fig. 1.1** continued

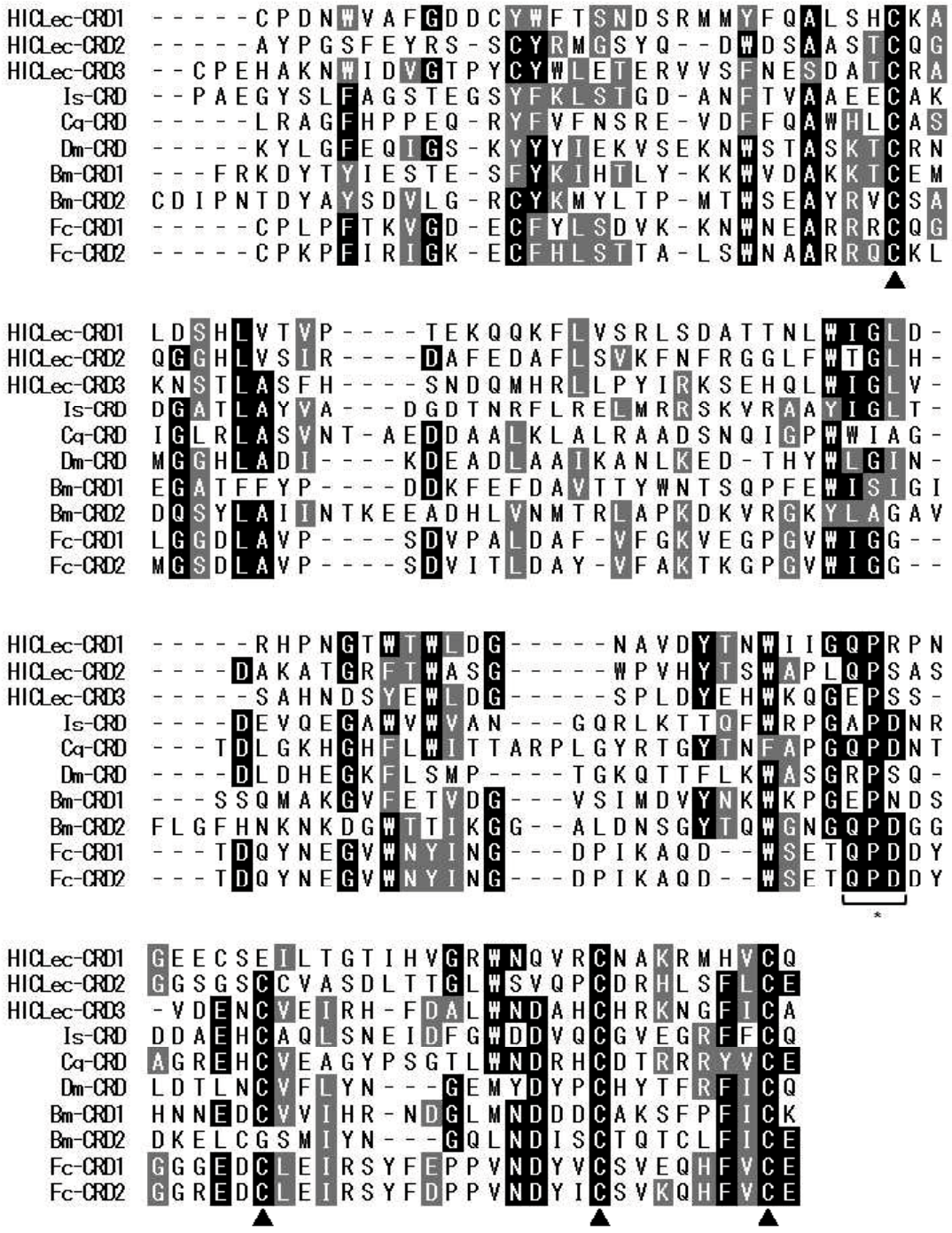


**Fig. 1.2** Multiple alignment of CRDs from other invertebrates made by Clustal W program. Identical and similar amino acid residues were shaded in black and gray. Asterisk shows conserved $Ca^{2+}$-binding site 2 motifs. Triangle presents highly conserved cysteine residues. Is: *Ixodes scapularis* (Accession no.: EEC15231.1), Cq: *Culex quinquefasciatus* (Accession no.: AAR18440.1), Dm: *Drosophila melanogaster* (Accession no.: ACL82973.1); Bm: *Bombyx mori* (Accession no.: BAF03496.1); Fc: *Fenneropenaeus chinensis* (Accession no.: AAX63905.1).

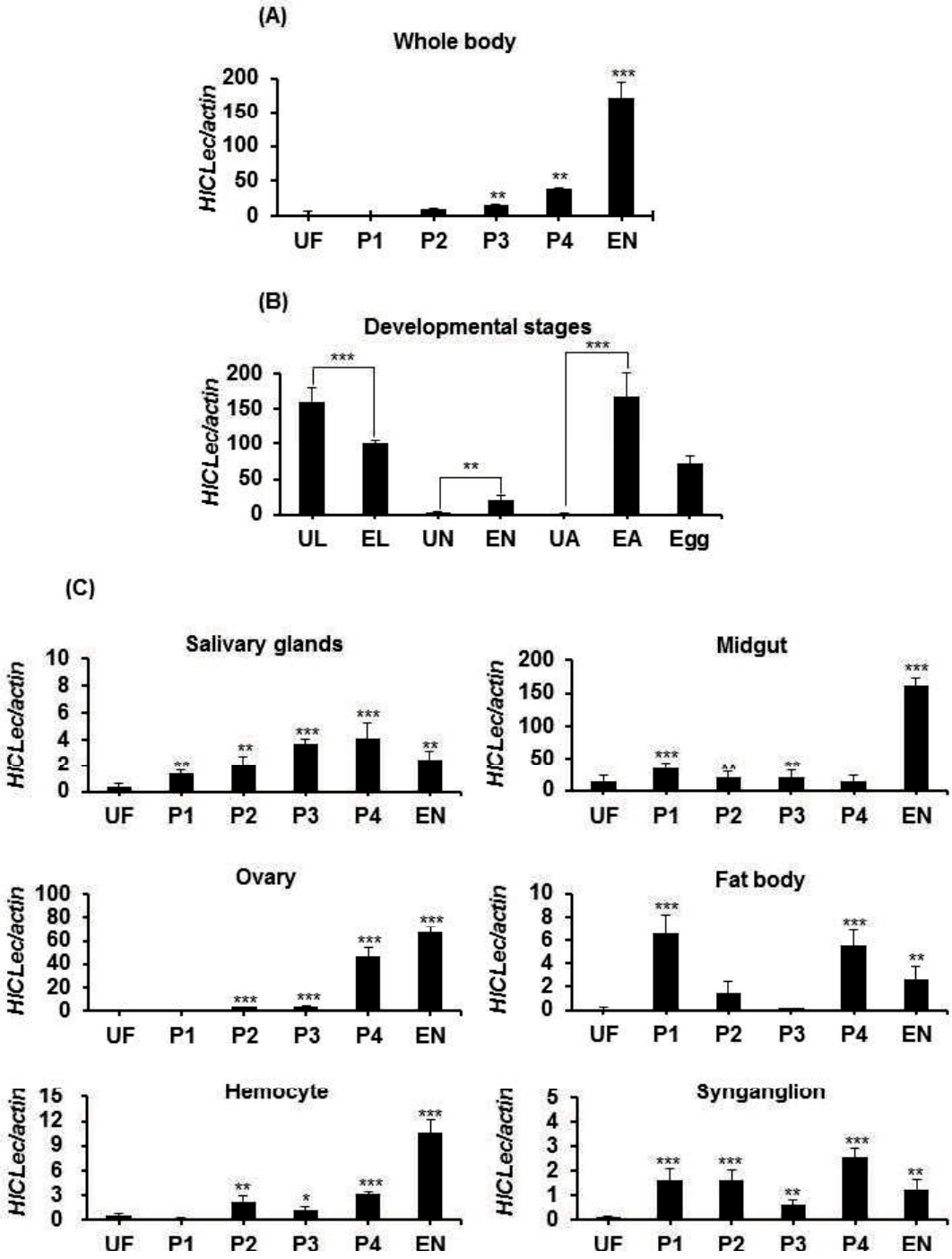


**Fig. 1.3** Transcription profiles of *HlCLec* analyzed by qPCR.

(A) in whole ticks. UF, unfed adults; P1-P4, adults partially fed for 1-4 days; EN, engorged adults. (B) in developmental stages. UL, unfed larvae; EL, engorged larvae, UN, unfed nymph; EN, engorged nymph; UA, unfed adults; EA, engorged adults.

(C) in different organs. UF, unfed adults; P1-P4, adults partially fed for 1-4 days; EN, engorged adults. **P*<0.05; ***P*<0.03; ****P*<0.01, significantly different by Mann-Whitney *U* test.

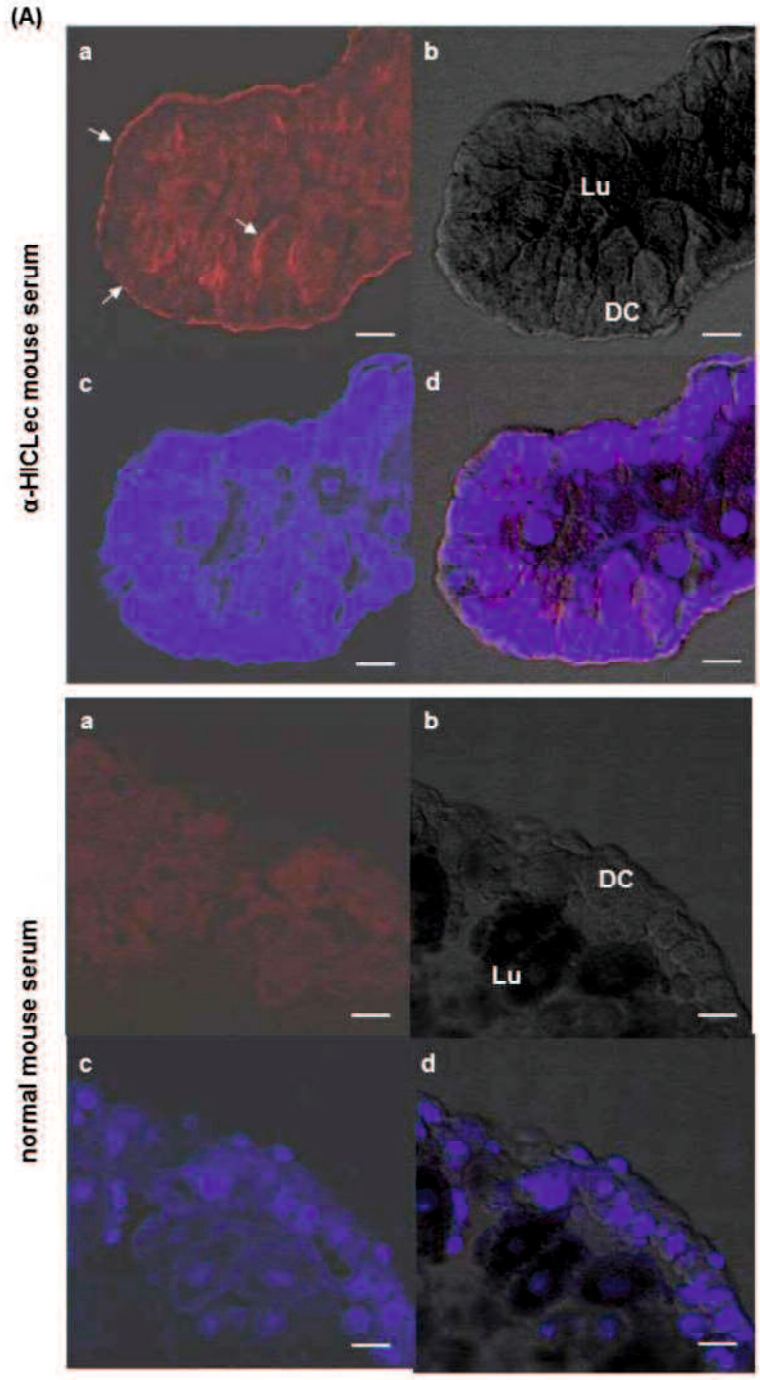


**Fig. 1.4** Examination of midgut and ovary from partially fed adult ticks by Indirect-fluorescent antibody test (IFAT) using a confocal laser scanning microscope. Anti-HlCLec was used for primary antibody, Anti-mouse IgG conjugated with Alexa 594 was used for secondary antibody and nuclei were visualized using DAPI. Normal mouse serum was used for control. a, Alexa 594; b, Differential interference contrast; c, DAPI; d, Merge; bar 20 μm (A) midgut. Lu, lumen; DC, digestive cells.

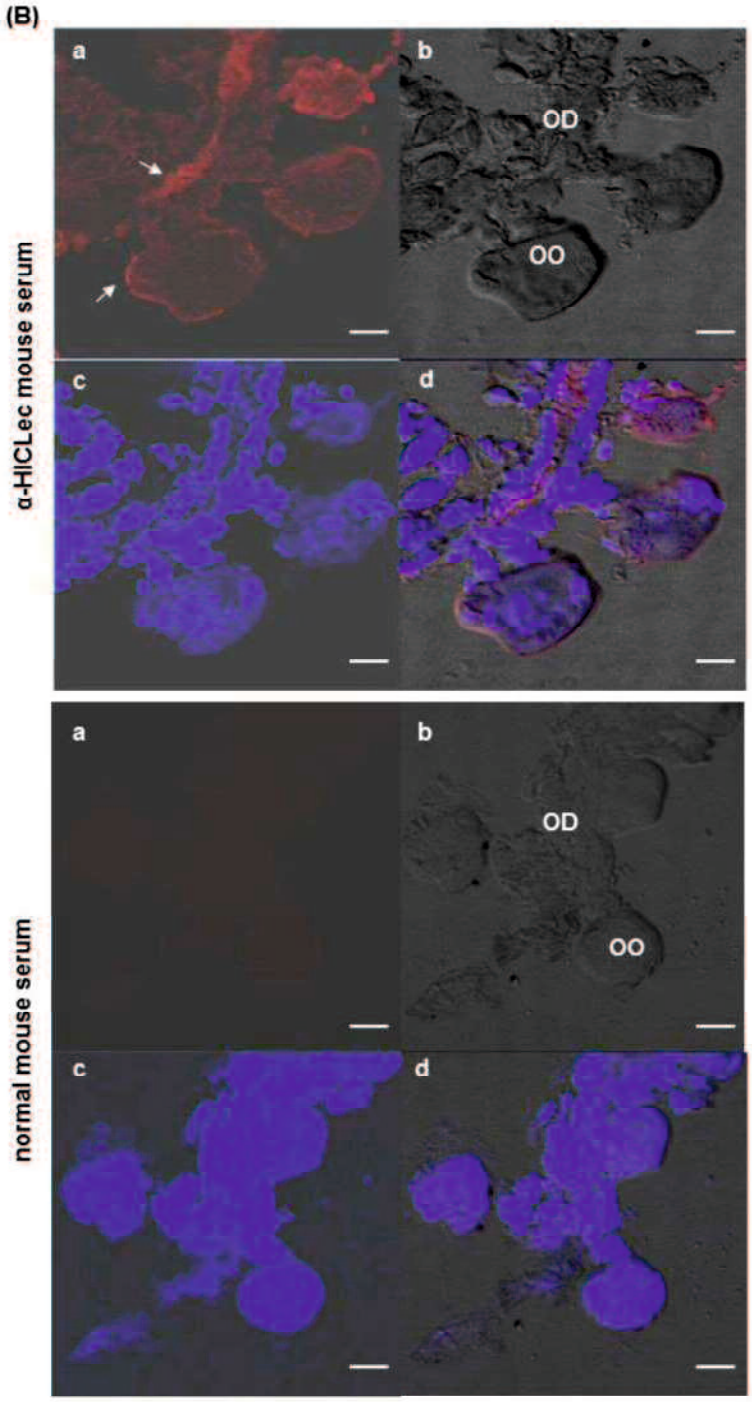


**Fig. 1.4** (B) ovary. OD, oviduct; OO, oocyte. Arrows show positive fluorescent of HlCLec.

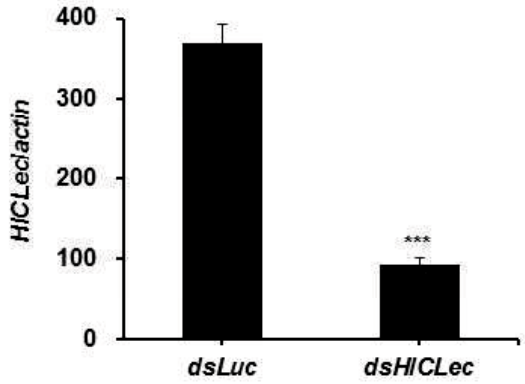


**Fig. 1.5** Confirmation of gene silencing of *HlCLec* by qPCR. Three days partially fed ticks were used for confirmation of gene silencing. The expression level of *HlCLec* were normalized by *actin*. ***$P$<0.01, significantly different by Mann-Whitney $U$ test.

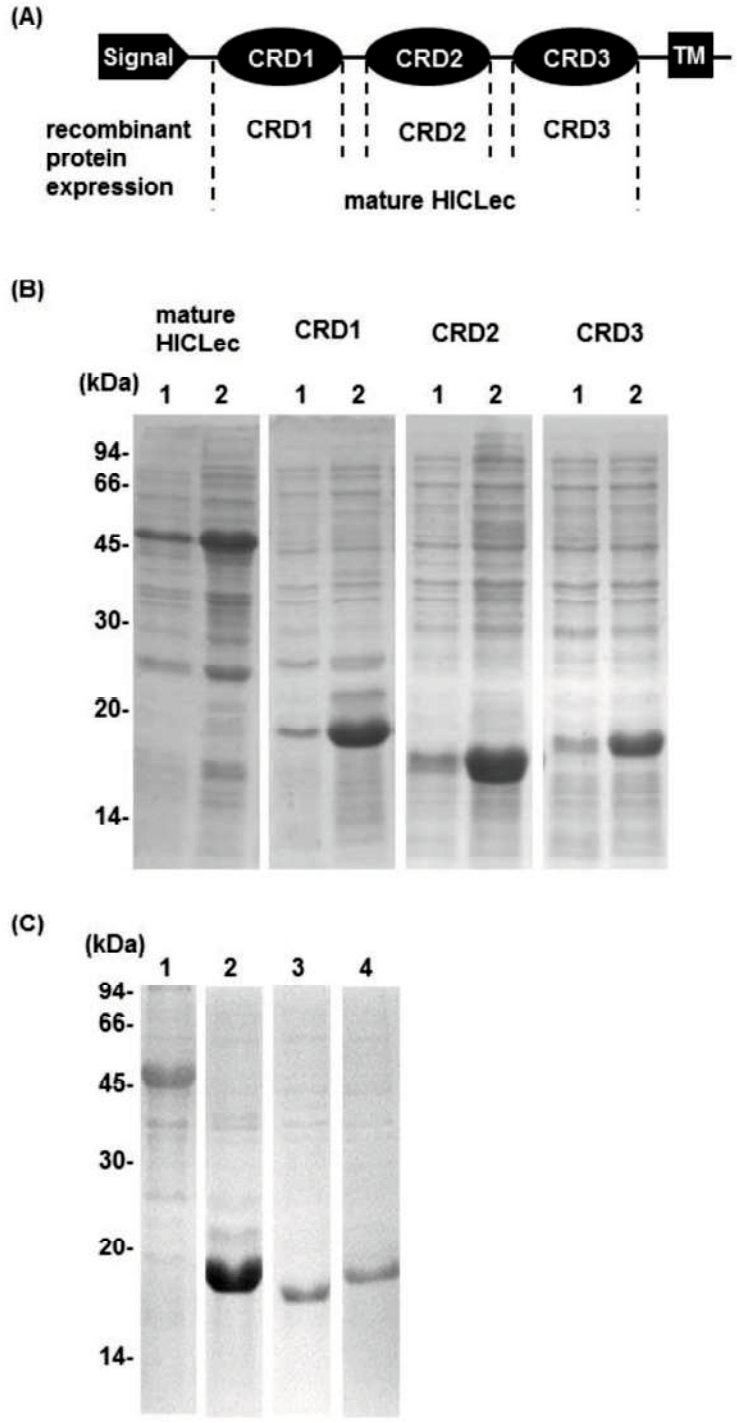


**Fig. 1.6** Expressed recombinant CRDs. (A) A diagram of the recombinant proteins expressed region. (B) SDS-PAGE analyses of expressed recombinant proteins. Lanes 1, *E. coli* lysate before IPTG induction; Lanes 2, *E. coli* lysate after IPTG induction. (C) Purified recombinant proteins. Lane 1, mature HlCLec; Lane 2, CRD1; Lane 3, CRD2; Lane 4, CRD3.

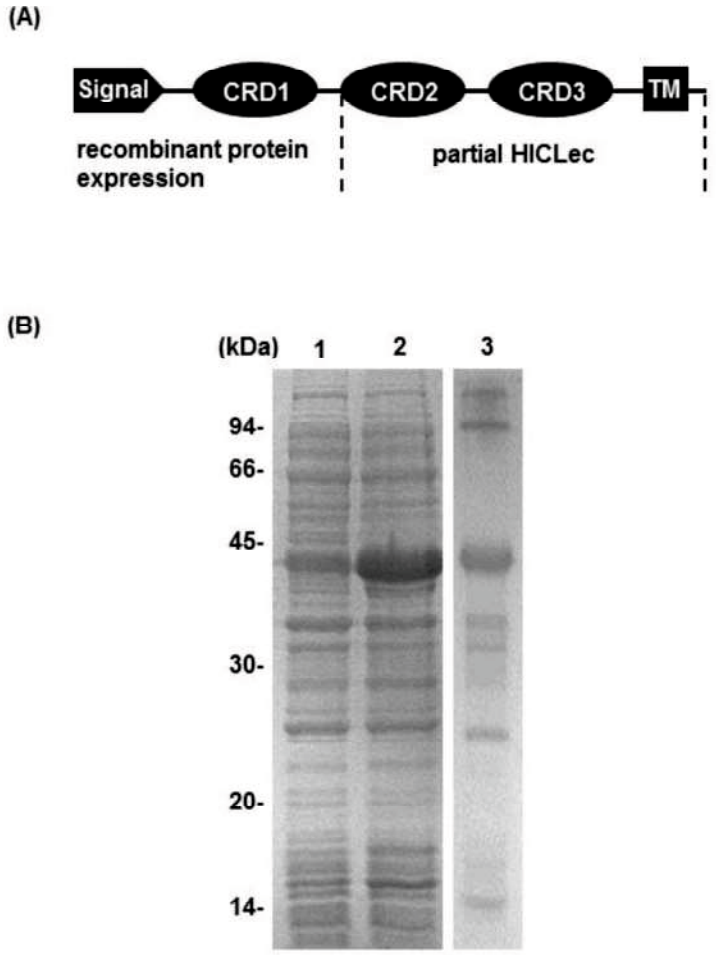


**Fig. 1.7** Expressed recombinant partial HlCLec. (A) A diagram of the recombinant partial HlCLec expressed region. (B) SDS-PAGE analyses of expressed and purified recombinant proteins. Lanes 1, *E. coli* lysate before IPTG induction; Lanes 2, *E. coli* lysate after IPTG induction; Lane3, purified partial HlCLec.

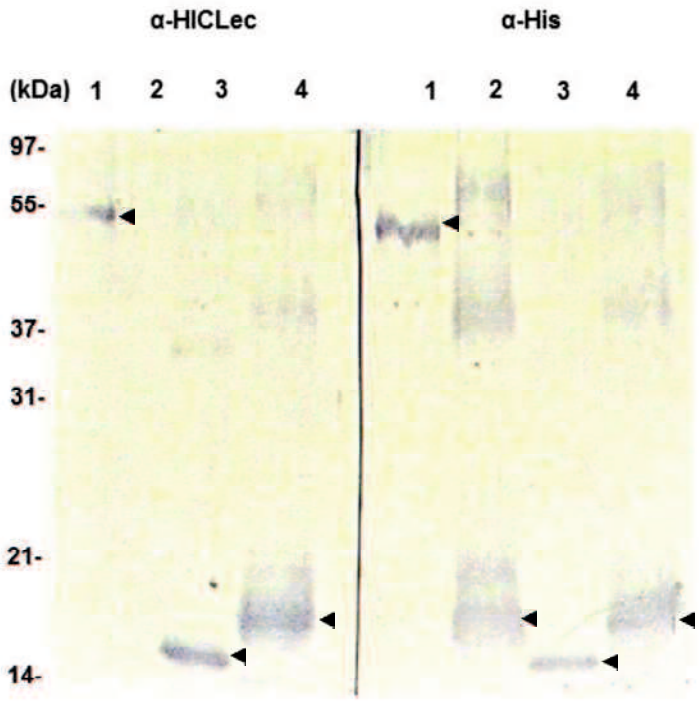


**Fig. 1.8** The specificity of the produced HlCLec antisera from mice. Lanes 1, mature HlCLec; Lanes 2, CRD1; Lanes 3, CRD2; Lanes 4, CRD3. Arrow heads show estimated bands as predicted from calculated molecular mass. Anti-His antibody was used as a control.

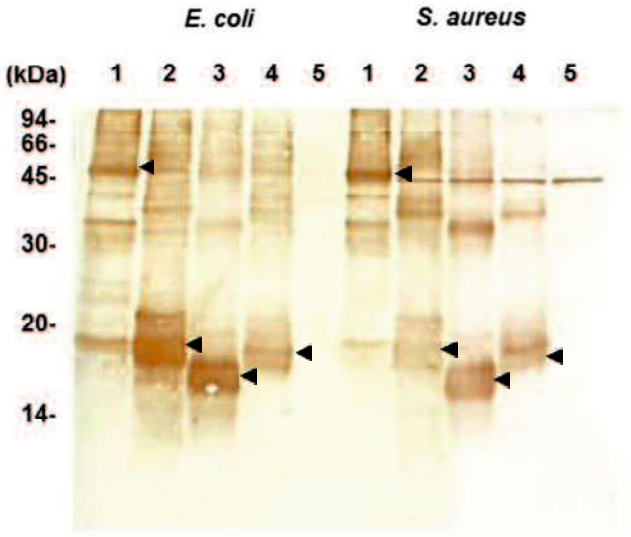


**Fig. 1.9** Direct bacterial binding assay to recombinant proteins. Recombinant proteins were incubated with bacterial suspension. After gently rotated at room temperature for 30 min, samples were centrifuged. The bacterial pellets were washed 5 times with TBS and eluted by 7% SDS and the lysates were applied on 15% SDS-PAGE for western blot analysis with anti-His antibody. Lanes 1, mature HlCLec; Lanes 2, CRD1; Lanes 3, CRD2, Lanes 4, CRD3; Lanes 5, COMP for negative control. Arrow heads show estimated bands as predicted from calculated molecular mass.

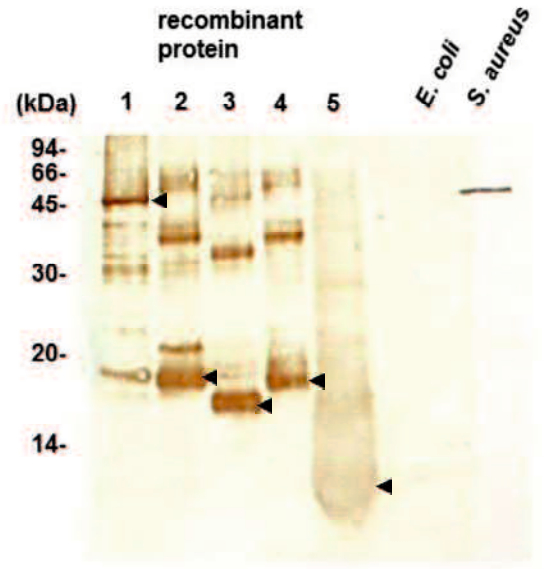


**Fig. 1.10** Positive and negative control for bacterial binding assay. Only recombinant proteins or bacterial lysates were used for western blot analyses. Lane 1, mature HlCLec; Lane 2, CRD1; Lane 3, CRD2; Lane 4, CRD3; Lane5, COMP for negative control. Arrow heads show estimated bands as predicted from calculated molecular mass.

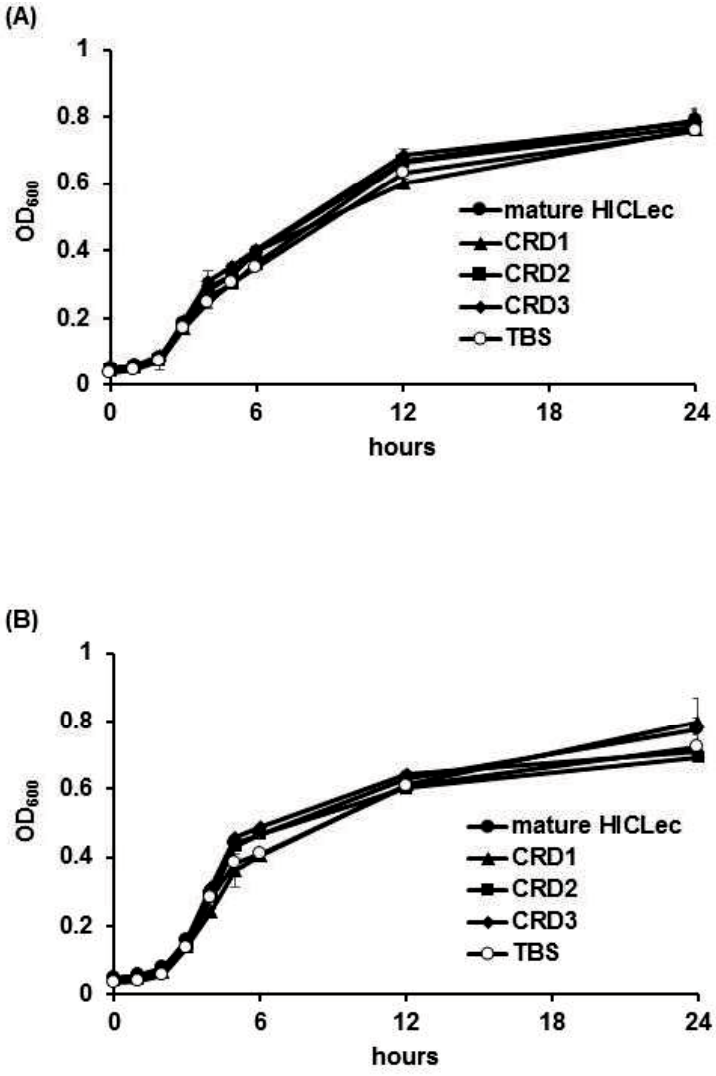


**Fig. 1.11** Bacterial growth inhibition assay. Bacteria were incubated with recombinant proteins in the TSB medium at 37°C and $OD_{600}$ were monitored every 6 h.
(A) *E. coli* (B) *S. aureus*.

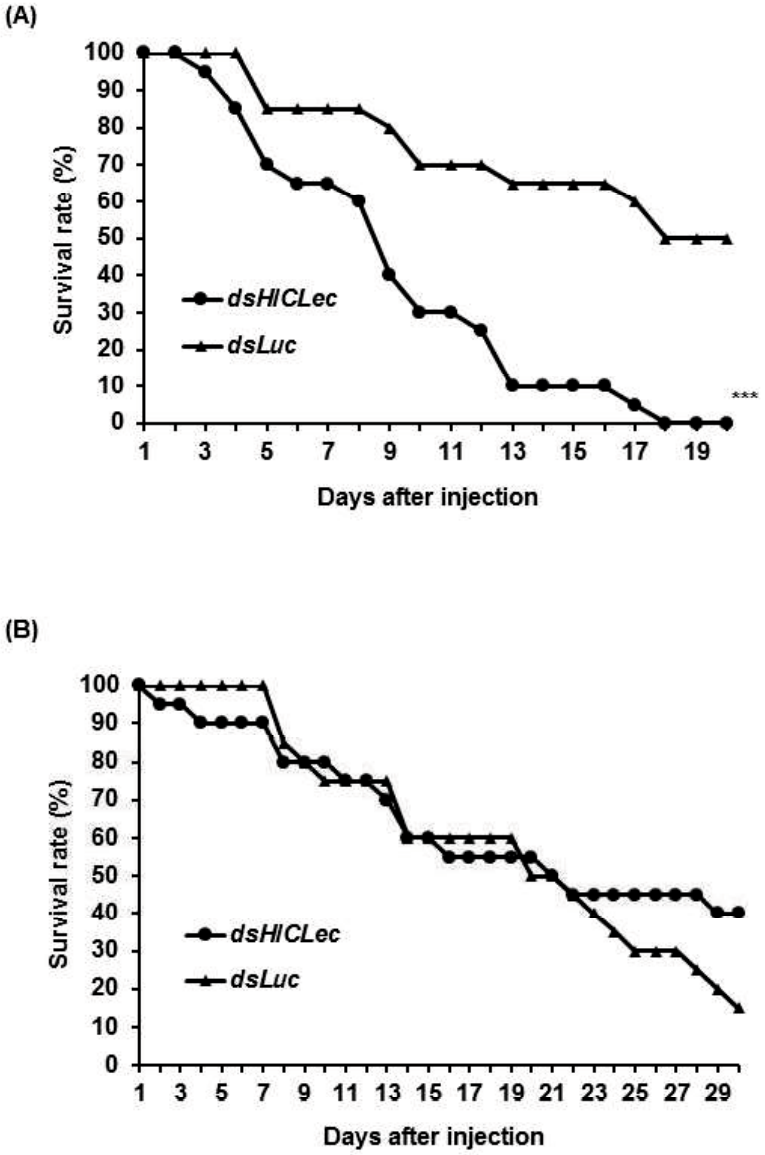


**Fig. 1.12** Gene silenced tick survival rate after bacterial injection. dsHlCLec or dsLuc was injected to unfed female adult ticks for each groups. The gene silenced ticks were allowed to infest on the rabbit in 3 days. Three days partially fed ticks were detached and *E. coli* or *S. aureus* ($2\times10^6$/ticks) was injected, then tick survival rate was monitored every day. (A) *E. coli* (B) *S. aureus.* ***$P$<0.01, significantly different by the log-rank test.

# CHAPTER 2

## The migration of *Babesia ovata* in *Haemaphysalis longicornis*

**This work has been published as:**

Maeda, H., Hatta, T., Alim, M.A., Tsubokawa, D., Mikami, F., Matsubayashi, M., Miyoshi, T., Umemiya-Shirafuji, R., Kawazu, S., Igarashi, I., Mochizuki, M., Tsuji, N., Tanaka, T. (2016). Establishment of a novel tick-*Babesia* experimental infection model. *Sci. Rep.*, ***6***, 37039.

## 2.1 Introduction

*B. ovata* is a benign intraerythrocytic protozoan parasite of cattle which is vertically (transovarially) transmitted by *H. longicornis*. It has been experimentally proved that transmission of *B. ovata* to cattle takes place by only the larval stage of *H. longicornis* [58] and it is considered that the larval stage of *H. longicornis* is the important stage for the transmission of babesiosis caused by *B. ovata*. Also, other cattle *Babesia* with high pathogenicity, including *B. bigemina* and *B. bovis*, were transmitted transovarially [59–61]. *B. ovata* causes no severe clinical symptoms and it is considered to be a model organism for investigating the tick stage of *Babesia*. For the advancement of the understanding of the relationship between the vector and vector-borne pathogens, laboratory experimental models as with mosquito and malaria parasite [62, 63] might be produced. Several studies on the lifecycle of *Babesia* parasites in ticks have been conducted; however, unlike malaria parasites [64], our knowledge about the time information for the development of *Babesia* parasites in the vector is still limited [65, 66]. Moreover, when using experimental animals such as cattle, tick-*Babesia* research is expensive and requires great efforts including the clinical management of animals and rearing ticks and the maintenance of *Babesia* parasites in the laboratory.

Tick artificial feeding (membrane feeding or tube feeding) is a widely used technique that is considered as an effective tool for producing ticks infected with parasites [67–69]. This technique mimics the natural process of feeding and reduces the host factors. To date, many studies on the tick-pathogen interaction based on the artificial feeding system have been conducted [70–72]. However, for monitoring the transmission speed of the parasites in the tick vector by these systems, it costs us lot efforts to obtain the engorged ticks because of their long artificial-feeding period. Generally, female ticks stop their blood feeding partially and wait to mate with male ticks. After mating, the female ticks resume feeding toward engorgement and laying eggs [73]. Due to their unique feeding process, it is hard to synchronize their engorgement. Here, I describe a novel tick-*Babesia* experimental infection model with *H. longicornis* and *B. ovata* using a semi-artificial feeding system [74]. In Chapter 2, I developed the quantification model for transovarially transmitted *Babesia* parasite in the vector ticks. This system is quite simple and we could obtain synchronous engorged tick experimentally infected with *Babesia* pathogens within 12-24 h of artificial feeding period. Through this model, it was possible to monitor quantitatively the transovarial transmission of *Babesia* parasites.

## 2.2 Materials and Methods

### *2.2.1 Ticks and mice*

The parthenogenetic Okayama strain of *H. longicornis* [11] was maintained by blood feeding on 6-month-old BALB/c mice (Japan SLC, Shizuoka, Japan) at the Department of Parasitology, Kitasato University School of Medicine. BALB/c mice were cared for in accordance with the guidelines approved by the Animal Care and Use Committee of Kitasato University (Approval No. 2015171). They were maintained in regulated conditions throughout the experiments.

### *2.2.2 In vitro culture of B. ovata*

The *in vitro* microaerophilus stationary phase culture system of *B. ovata* (Miyake strain) established by Igarashi et al. [75] was slightly modified to reduce the unknown factors in the bovine serum. GIT (Nihon Pharmaceutical Co., Ltd., Tokyo, Japan) instead of bovine serum and M199 medium (Sigma-Aldrich) were used as the mixture with a ratio of 2:3. Fresh bovine blood was purchased from Nippon Bio-Test Laboratories Inc. (Tokyo, Japan) to prepare the red blood cells (RBCs) [76]. The culture was maintained at 37°C with 5% oxygen and 5% carbon dioxide. Giemsa-stained blood smears were

examined daily to determine the parasitemia, which was calculated as the percentage of parasitized RBCs for 1,000 total RBCs counted. *B. ovata*-infected RBCs of approximately 1–2% parasitemia were used to feed ticks artificially.

### *2.2.3 DNA extraction from artificially engorged tick organs*

To prepare the mouse skin membrane, female adult ticks were allowed to feed on the shaven back of BALB/c mice. Eight to ten ticks were attached on each mice. After 4 to 5 days (at the beginning of the expansion period), a rectangular section of the mouse skin with the ticks attached was carefully removed from the mouse's body immediately after euthanasia, and set on the artificial feeding units [74]. Inside of the membrane was washed with sterilized PBS supplemented with 100 units/ml penicillin and 100 μg/ml streptomycin (Life Technologies Corporation, Carlsbad, CA). The ticks were fed on the RBC solution, composed of the fresh media and *B. ovata*-infected RBCs at a ratio of 7:3, using the artificial feeding units. To serve and maintain the fresh parasites in the system, the RBC solution that included *B. ovata* was changed every 12 h during tick feeding. Engorged and dropped ticks (19 from the experiment with approximately 1% parasitemia of *B. ovata* or 20 from the experiment with approximately 1.5% parasitemia) were obtained, and 3–4 of them were dissected daily from 0 to 4 days post engorgement (DPE)

to pick off the midgut, ovary, and carcass that included other organs. These organs were rinsed with PBS and immediately put into the DNA extraction buffer to extract the DNA as described previously [76]. The concentration of purified DNA was determined by NanoDrop 2000 (Thermo Scientific, Waltham, MA, USA) and then diluted at 50 ng/μl and stored at -30°C until use.

### *2.2.4 PCR detection of B. ovata DNA in the tick*

A specific primer set for *B. ovata β-tubulin* gene [77] (Table 2.1) was used in this study. For conventional PCR, KOD-Plus-Neo (Toyobo) was used. The cycling conditions were as follows: initial denaturation at 95°C for 2 min, followed by 40 cycles of denaturation at 98°C for 10 sec, annealing at 60°C for 30 sec, extension at 68°C for 15 sec, and final extension at 68°C for 7 min. qPCR was also performed with LightCycler 1.5 (Roche, Basel, Switzerland) using KOD SYBR qPCR Mix (Toyobo). For the standard templates, the *B. ovata* β-tubulin fragment was cloned into the pTA2 vector (Bo β-tub/pTA2) using a Mighty TA-cloning Kit (TaKaRa, Shiga, Japan). The cloned sequence was confirmed using the DNA-sequencing service of FASMAC Co., Ltd. (Kanagawa, Japan). To linearize the super-coiled plasmids, the plasmid DNA was treated with a *Bam*HI restriction enzyme (Toyobo). The copy number of 1 μg of the plasmid DNA was

calculated as the result of $9.1\times10^{11}$ divided by the size of plasmid DNA (kb). The standard template was a series diluted 10-fold with 50 ng/μl of tick DNA. The PCR cycling steps were as follows: initial denaturation at 98°C for 2 min, followed by 40 cycles of denaturation at 98°C for 10 sec, annealing at 60°C for 10 sec, and extension at 68°C for 30 sec. For the tick internal control, HlITS2 was used, as reported previously [78] (Table 2.1). The parasite burden was quantified as the ratio of the amplicon of the *B. ovata* β-tubulin fragment to the tick HlITS2 fragment for each sample. All test samples and plasmid standards were assayed in duplicate. For each PCR template, 50 ng of DNA/reaction was used. The detection rate was calculated as the percentage of the number of quantified samples in each group.

### *2.2.5 Recombinant protein expression of B. ovata P29*

The predicted P29 homologous fragments were amplified from *B. ovata* cDNA using the result of RNA sequencing from the midgut of *B. ovata*-infected ticks at 3 DPE (unpublished data). After confirming the sequencing (Fig. 2.3, FASMAC Co., Ltd.), the sequence was cloned into the pRSET B vector (Invitrogen) using an In-Fusion® HD Cloning Kit (TaKaRa) with a specific primer set (Table 2.1). For In-Fusion cloning, the pRSET B vector was digested with *Bam*HI and *Hin*dIII restriction enzymes (Toyobo) and

purified with the MinElute Gel Extraction Kit (Qiagen).

The recombinant plasmid was transformed in Rosetta™ (DE3) Competent Cells (Novagen, Darmstadt, Germany) and expressed by induction with 1 mM IPTG at 37°C for 4 h. The expressed recombinant protein was purified using the ProBond Purification System (Invitrogen) from the insoluble fraction under denaturing conditions. The purified recombinant protein was dialyzed against the PBS solution for refolding. The purity of the recombinant proteins was checked by SDS-PAGE. The concentrations of recombinant proteins were determined by a Micro BCA™ Protein Assay Kit (Thermo Scientific) and stored at -30°C until use.

### *2.2.6 Production of an anti-serum against B. ovata P29*

To prepare mouse anti-BoP29 sera, 100 μg of recombinant BoP29 completely mixed with TiterMax Gold Adjuvant (Sigma-Aldrich) was subcutaneously injected into BALB/c mice (Japan SLC). After 2 weeks, these mice were injected again to boost the generation of antibodies. Whole blood was collected from the mice 2 weeks after the second immunization to obtain the specific antisera for BoP29.

### *2.2.7 Visualization of B. ovata in the tick*

IFAT using tick section was performed as described previously [79]. Briefly, ticks were fixed overnight in a 4% paraformaldehyde phosphate buffer solution (pH 7.4) that included 0.1% glutaraldehyde and was embedded in paraffin. Cut sections were fixed on glass slides and deparaffinized in xylene. The sections were rehydrated with a graded series of alcohol and PBS, followed by trypsin treatment. They were then blocked using Blocking One Histo (Nacalai Tesque, Kyoto, Japan). They were then incubated for 1 h at 37°C with mouse anti-BoP29 serum (1:100) diluted by Can Get Signal Immunostain Immunoreaction Enhancer Solution (Toyobo). Sections treated with pre-immune mouse sera (1:100) were used as a control. After washing, sections were reacted with Alexa Fluor 488 goat anti-mouse IgG as a secondary antibody (1:1000) and mounted with VECTASHIELD Mounting Medium with DAPI (Vector Laboratories). The slides were examined under a confocal laser scanning microscope (LSM 710, Carl Zeiss, Oberkochen, Germany). For the IFAT with egg squashed smear, randomly selected eggs of 10 days post oviposition were used and treated as described previously [78].

## 2.3 Results

### *2.3.1 B. ovata migration in ticks*

The conventional PCR results in Fig. 2.2 show the existence of *B. ovata β-tubulin* DNA in the tick organs collected at the indicated days after their engorgement. The positive bands of *B. ovata* in the midgut samples seemed to gradually disappear after 1 DPE. On the contrary, those in the ovary and carcass were likely to increase after 1 DPE. Two independent trials showed the same tendency. To quantify the parasite burden in the samples, qPCR was also conducted. Initially, I verified the sensitivity of the qPCR and confirmed the typical amplification curve, melting curve with no primer dimerization, and correlative standard curve using the artificially prepared meta-genomic DNA samples, including the plasmid DNA-carrying *B. ovata β-tubulin* fragment and tick genomic DNA (Fig. 2.1). The developed qPCR system was able to detect and quantify the parasite DNA in some samples; however, the values of the parasite burden in the qPCR-positive samples were quite low and did not show any correlation between their values and body weight (Table 2.2). However, the detection rate calculated from the results of qPCR showed the same tendency as the results of conventional PCR. The detection rate in the midgut at 0 DPE was 100%, that decreased to 25% at 1 DPE and onward. In contrast, the detection

rate in the ovary and carcass samples reached to 75–100% at 1 DPE and onward (Fig. 2.2). These results imply that *B. ovata* might pass through the midgut epithelium within 24 h after tick engorgement.

### *2.3.2 Localization of Babesia parasites in tick organs*

To detect the parasite in the ticks specifically, *B. ovata* P29 (BoP29; Accession No. LC110193; Fig. 2.3), homologous to a cytoskeleton protein and conserved among the other apicomplexan protozoa including *Toxoplasma gondii* [80] and *B. gibsoni* [81] was selected as marker for the IFAT. P29 protein is one of the important cytoskeleton proteins in the apicomplexan parasites and, thus, is considered to be their constitutive protein. Six histidine-tagged recombinant BoP29 were expressed using *E. coli* for the preparation of specific antisera against BoP29 (Fig. 2.4A). As shown in the immunoblotting result (Fig. 2.4B), the anti-BoP29 mouse serum detected a clear 29-kDa single band in the lysate of *B. ovata*-infected RBCs. Furthermore, anti-BoP29 specifically reacted with a fiber-like structure of the *B. ovata* merozoite in the parasitized RBCs on the blood smear (Fig. 2.5). In the tick sections, dot-like reactions identical to reactions to the body parts of *B. ovata* parasites were detected in the tick cells or hemocoel (Fig. 2.6). This suggests that because the sections were cut, positive fluorescence indicating BoP29 was detected in the cells

and in the hemocoel apart from other organs. It was limited in that I could not identify the origin of the cells; furthermore, detection of the complete form of *B. ovata* parasites was difficult. As shown in the previous report [78], spherical cells with a positive signal were also observed in the egg squashed smear (Fig. 2.6), which strongly suggests that *B. ovata* infected *H. longicornis* ticks and transovarially migrated to their eggs.

## 2.4 Discussion

The three-host tick, *H. longicornis*, is very useful and suitable for studying the transovarial transmission of *Babesia* parasites, because this tick has a unique thelytokous parthenogenetic characteristic. This tick does not need to mate for its engorgement and reproduction [73]. *H. longicornis* is easy to maintain and is widely used as a model tick to study pathophysiology in tick infestation [82]. To date, a number of bioactive molecules have been found in *H. longicornis*, and those products might be available for not only tick control but also for novel drug discovery in the veterinary and medical fields [12, 13, 76, 79, 83]. The experimental infection of ticks with pathogens is considered to be an attractive tool for studying tick-pathogen interaction [6, 7]. In the present study, a novel tick-*Babesia* experimental model was established and validated. Interestingly, a

reverse phenomenon for the detection rate of *B. ovata* of the midgut sample as compared with the ovary/carcass samples was observed at 1 DPE. In some studies, a positive correlation between the blood parasite levels of infected animals and the kinete level of *Babesia* in the hemolymph of the dropped tick has been shown [10, 60, 61]. I applied *B. ovata*-infected RBCs with parasitemia of 1–2%, which was assumed to be approximately 100 times higher than that of the natural condition (less than 0.01%) [10]. Nevertheless, *B. ovata* DNA in some samples was not detected by qPCR. This might be caused by significant *in vitro* passage of *B. ovata*, resulting in phenotypic changes regarding the ability of parasites to infect the vector tick, as described in previous articles [84–86]. In accordance with these evidences, I hypothesized that most *Babesia* parasites might pass through the midgut barrier within 24 h after tick engorgement, and the direction of their migration at the midgut epithelium might be one way (Fig. 2.7). Gough et al. [87] showed a time-course model of a stage transition of *B. bigemina* in the midgut lumen of its vector tick, *Rhipicephalus* (*Boophilus*) *microplus*. They cultured merozoites of *B. bigemina in vitro* with the midgut extract from the engorged female ticks and showed that its development from the merozoite to the zygote finished within 7.5 h post cultivation. Bock et al. [88] reviewed that the zygote selectively infects the digestive cells and vitellogenic cells of the tick midgut and that its multiplication probably occurs in those cells to develop

kinetes that move into the tick hemolymph. These reports partly support my hypothesis that 24 h after engorgement is considered as an important window for the migration of *B. ovata* in the tick lumen. In addition, I detected the *B. ovata* DNA from tick ovaries and *Babesia* parasites in the *B. ovata*-infected tick eggs, which supported the transovarial transmission of this parasites (Fig. 2.2, 2.6). Higuchi et al. [89] first detected the *B. ovata* from ovary and eggs of *H. longicornis* dropped from the *Babesia*-infected cattle. They detected kinetes for the first time at 6 DPE. However, as shown in the Fig. 2.2, qPCR-based assay proved that after 1 DPE, tick ovary gradually become pathogenic. It is considered that this system is more sensitive than the microscopic method. I also observed the round-formed bodies of *Babesia* parasites in the tick eggs as previously reported [78, 89]. The morphological changes of *Babesia* parasites were also detected in the midgut of nymphal stages of *H. longicornis* fed on infected cattle by Higuchi et al. [90]. The similar development of *Babesia* parasites was observed in the midgut of artificially-engorged adult ticks in this study, and will be detail-described in Chapter 3. The successful development and migration of *B. ovata* in ticks indicated that the *in vitro* cultured pathogens conserved the transmission ability.

A novel system for evaluating the interaction between *B. ovata* and its vector tick, *H. longicornis*, has been developed. This method is considered to be quite simple

and cost effective and could be used to monitor and quantify the infection level of *B. ovata* in tick organs with high sensitivity. This experimental model would be a powerful tool for clarifying the kinetics of the tick stage of *Babesia* parasites. With the rapid progress of genome-editing strategies, transgenic organisms are currently available as attractive tools to aid in molecular and cellular studies of *Babesia* and *H. longicornis* [82, 91]. Precise study of tick-*Babesia* molecular interactions using this developed model will also give us concrete knowledge to develop novel strategies for controlling babesiosis.

## Tables and Figures in CHAPTER 2

Table 2.1 Gene-specific primers used in Chapter 2

| Primer | Sequence (5'→3') |
|---|---|
| Bob-tub F[a)] | ACACTGTGCATCCTCACCGTCATAT |
| Bob-tub R[a)] | CTCGCGGATCTTGCTGATCAGCAGA |
| HlITS2 F[b)] | GCGTGTTGGGAAGTCTGAA |
| HlITS2 R[b)] | CGCGGTTTACGAGAGAAAG |
| BoP29 in-fusion F | ATGACGATAAGGATCCGATGCAGTGCTGTTCTAGGG |
| BoP29 in-fusion R | GCCAAGCTTCGAATTTTAAGCAGTTGCCTCGGG |

[a)]Sivakumar et al., 2014 [77]; [b)]Hatta et al., 2012 [74]

Table 2.2 Parasite burden of *B. ovata* in tick organs

| DPE | Experiment 1 | | | | | Experiment 2 | | | | |
|---|---|---|---|---|---|---|---|---|---|---|
| | Tick ID | BW (mg) | MG | OV | CA | Tick ID | BW (mg) | MG | OV | CA |
| 0 | #1 | 123.3 | + | ND | ND | #1 | 105.1 | + | ND | + |
| | #2 | 120.9 | + | ND | ND | #2 | 92.8 | + | + | ND |
| | #3 | 214.7 | + | ND | ND | #3 | 235.9 | ++ | ND | + |
| | | | | | | #4 | 181.4 | + | ND | + |
| 1 | #4 | 220.9 | ND | ND | ++ | #5 | 147.1 | ND | ND | + |
| | #5 | 241.4 | ND | + | + | #6 | 151.4 | ND | ++ | ++ |
| | #6 | 159.6 | ND | ++ | + | #7 | 179.9 | ND | +++ | + |
| | #7 | 150.2 | ++ | ++ | ++ | #8 | 202.8 | + | ++ | + |
| 2 | #8 | 188.5 | ND | ND | + | #9 | 154.1 | ND | + | + |
| | #9 | 277.4 | ++ | ND | + | #10 | 186.1 | ND | ND | + |
| | #10 | 145.9 | ND | + | + | #11 | 211.3 | ND | ++ | + |
| | #11 | 183.6 | ND | ++ | ND | #12 | 193.5 | + | ++ | + |
| 3 | #12 | 165.2 | ND | + | ND | #13 | 230.2 | ND | ND | ND |
| | #13 | 139.4 | ++ | + | ++ | #14 | 199.1 | ND | ++ | ND |
| | #14 | 173.4 | ND | + | + | #15 | 191.6 | ND | ++ | ++ |
| | #15 | 184.6 | ND | ++ | ND | #16 | 267.5 | + | ++ | + |
| 4 | #16 | 265.9 | ND | ++ | ++ | #17 | 274.3 | ND | + | ++ |
| | #17 | 166.6 | ND | + | + | #18 | 229.3 | ND | + | ++ |
| | #18 | 160.9 | ND | ND | + | #19 | 220.5 | + | + | ++ |
| | #19 | 127.9 | ++ | ++ | ++ | #20 | 253.1 | ND | ND | + |

The quantified copy number of the *B. ovata β-tubulin* gene was normalized by the tick *ITS2* gene. The quantified value was presented as +, $10^{-9}$~$10^{-6}$; ++, $10^{-6}$~$10^{-3}$; +++, $10^{-3}$~$10^{0}$. ND, not detected.

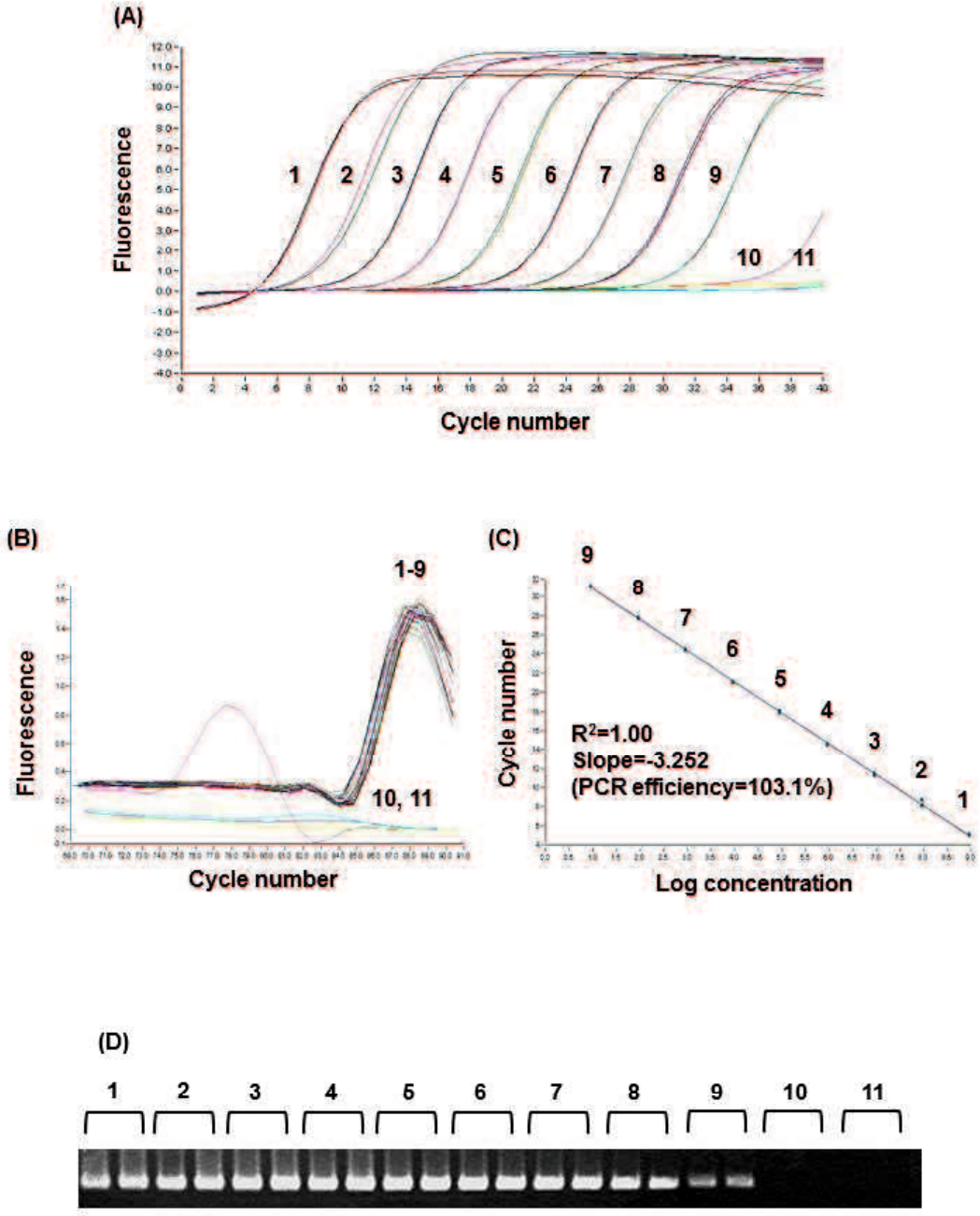


Fig. 2.1 Sensitivity of qPCR. To confirm the detection limit of qPCR, a 10-fold serial dilution of Bo β-tub/pTA2 was used for a template. Tick DNA and water were also used for a negative control. (A) Amplification curve; (B) Melting curve; (C) Standard curve; (D) Gel electrophoresis of the PCR products. 1–9, 10-fold serial dilutions of Bo β-tub/pTA2 plasmids mixed with tick genomic DNA; 10, tick DNA; 11, water sample.

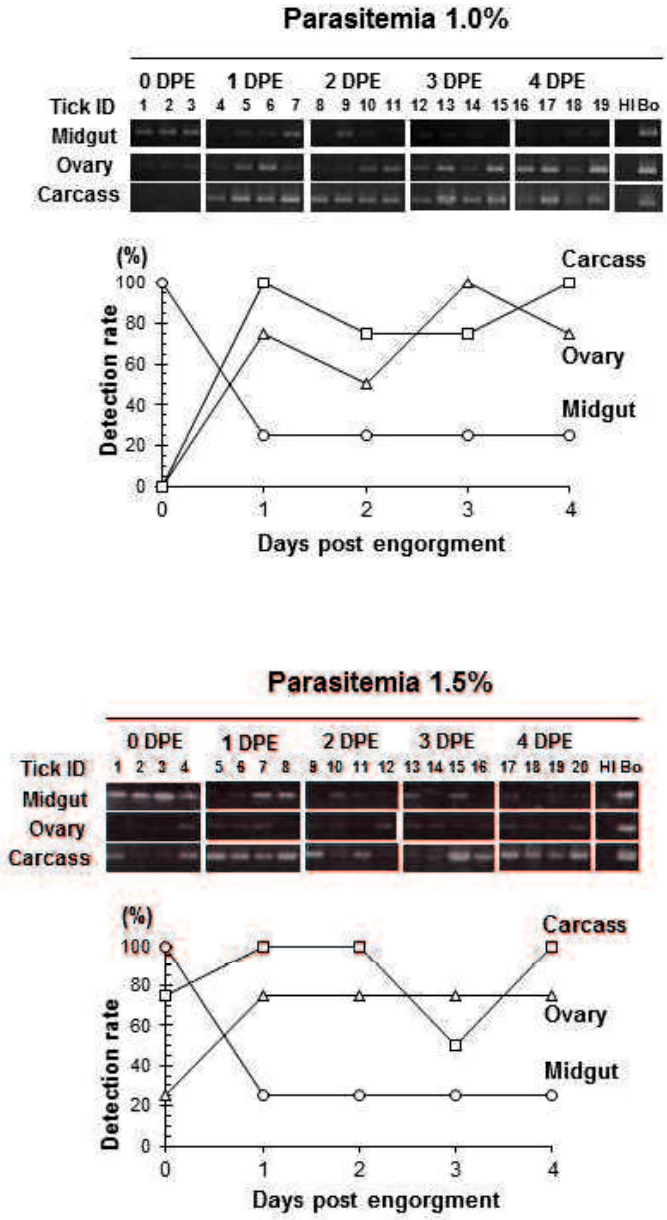


Fig. 2.2 Results of two experiments for the detection of *B. ovata* in tick organs. The top figure shows the conventional PCR. The lower line graph indicates the percentage of countable samples from qPCR. The same concentration of DNA was used for each sample. Tick and *B. ovata* DNA was prepared for negative and positive controls. DPE, days post engorgement; Hl, *H. longicornis*; Bo, *B. ovata*; 1–20, Tick ID No.

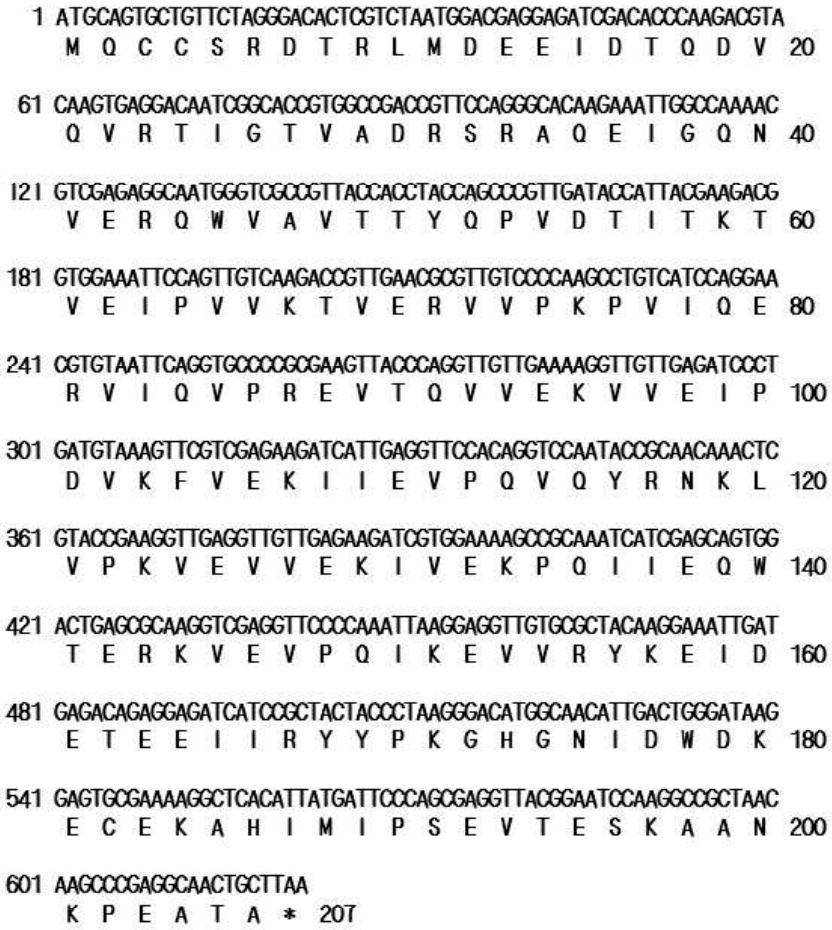


Fig. 2.3 Cloned P29 ORF sequences from *B. ovata.* Cloned BoP29 ORF consists of 621 bp encoding 206 amino acids and shows high homology with *B. bigemina* P29 (99%), *B. bovis* P29 (93%), and *B. gibsoni* P29 (89%).

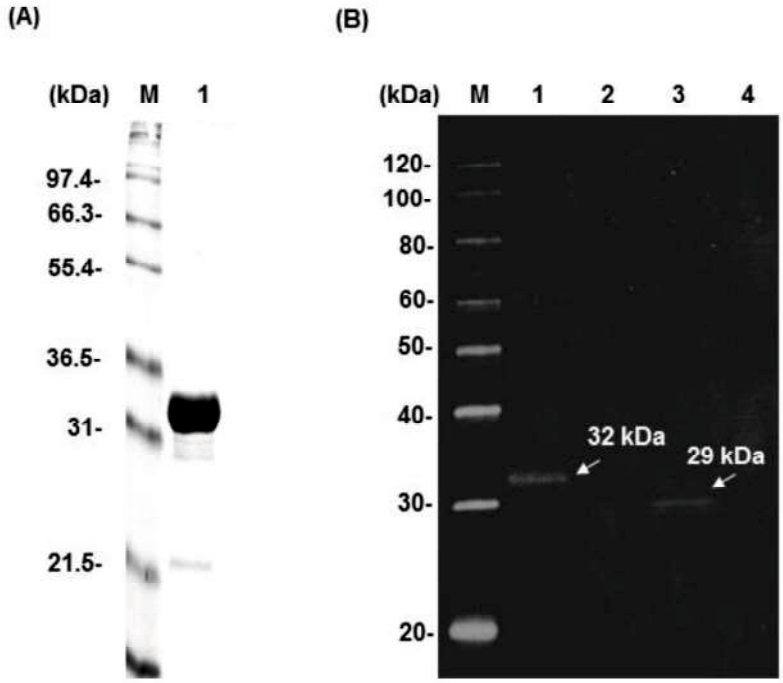


Fig. 2.4 Preparation of recombinant BoP29 for the generation of a specific anti-sera.
(A) Purified recombinant BoP29 loaded in 15% SDS-PAGE gel.
(B) Sensitivity and specificity of anti-BoP29 mouse serum by western blotting.
Lane 1: purified recombinant BoP29; Lane 2: *E. coli* lysate with expression vector;
Lane 3: lysate of *B. ovata*-infected RBCs; Lane 4: lysate of normal RBCs.

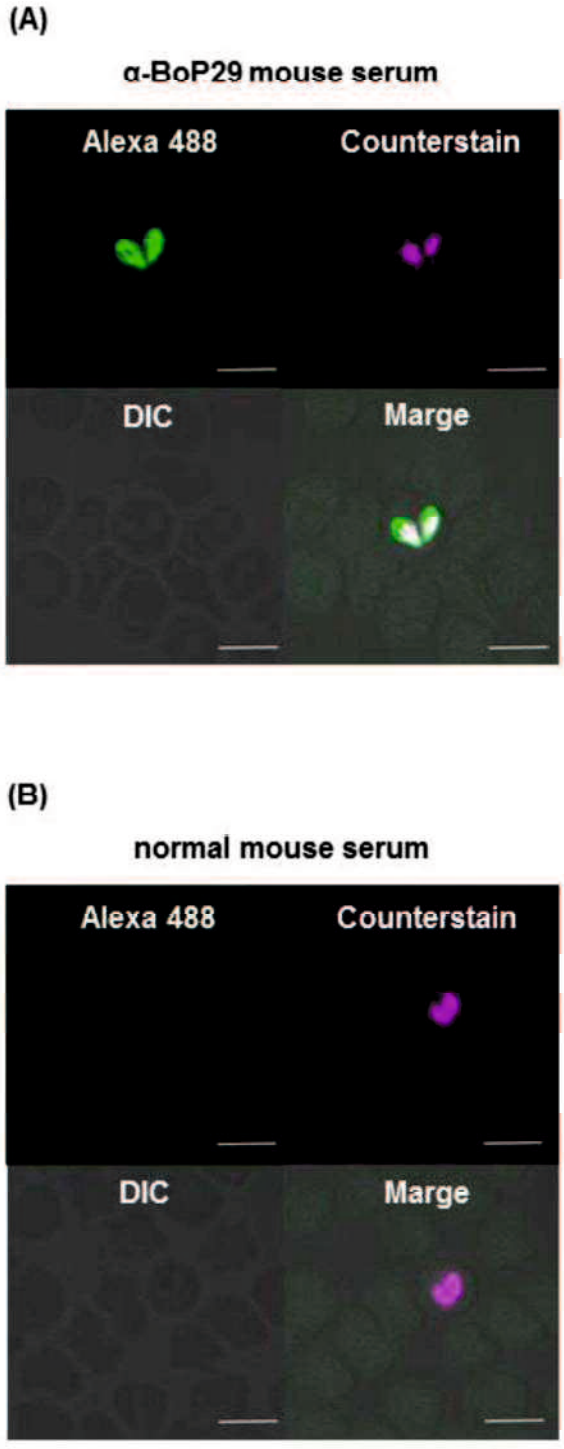


Fig. 2.5 IFAT of *B. ovata*-infected RBCs
(A) anti-BoP29 mouse serum (B) normal mouse serum. Bar: 5 μm

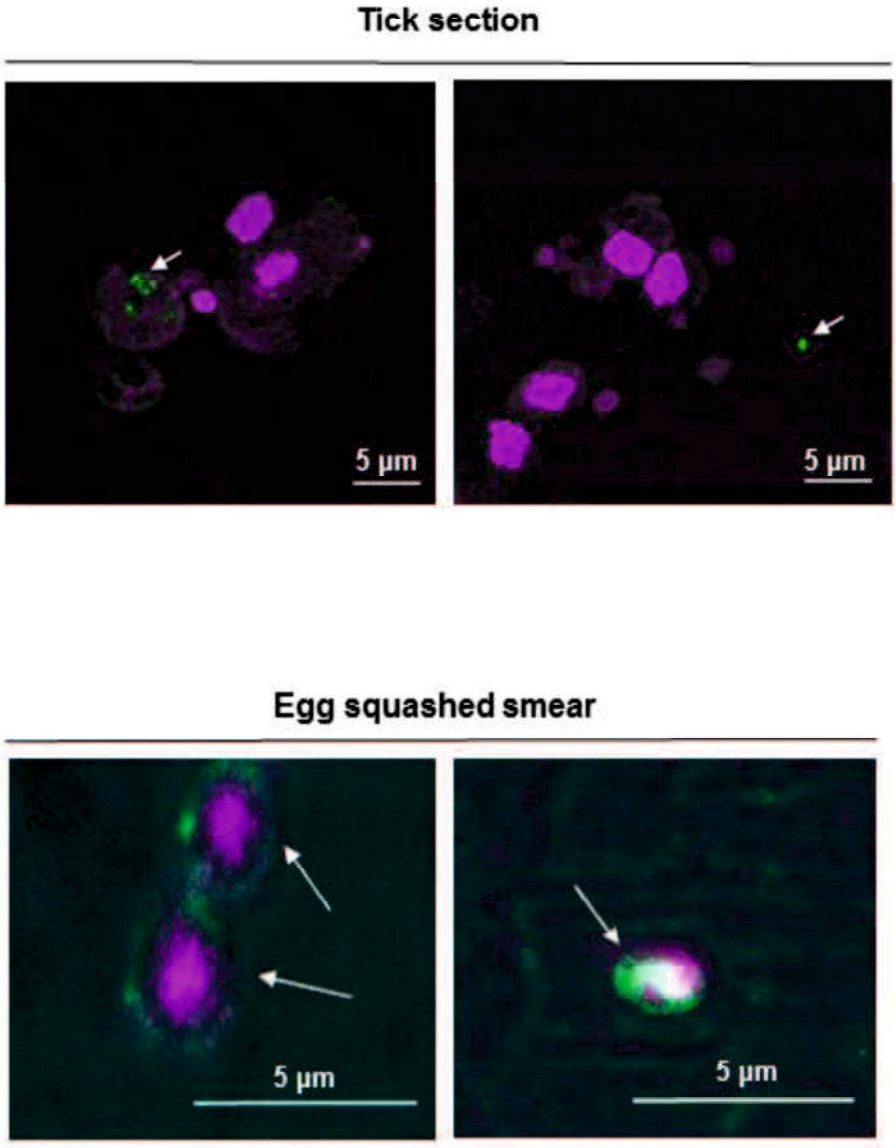


Fig. 2.6 IFAT of *B. ovata* in the tick samples. The two upper panels show *B. ovata* in the tick sections. Arrows indicate the *B. ovata*. The two under panels show *B. ovata* parasites (arrows) in the egg squashed smears. Bar: 5 µm

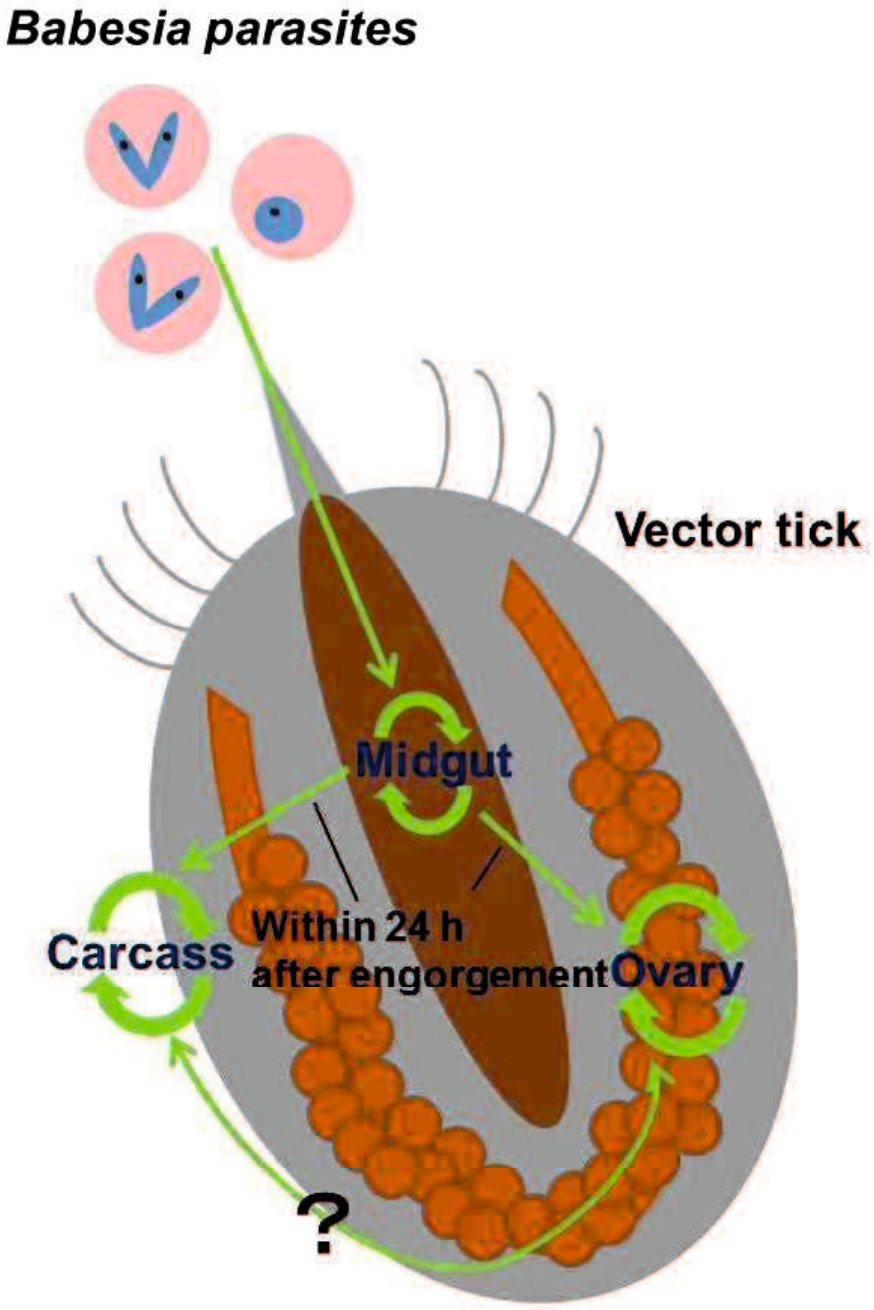


Fig. 2.7 Conclusive figure. Green arrows show the migration kinetics of *B. ovata*. *B. ovata* might pass through the midgut epithelium within 24 h after tick engorgement, and then proliferation will occur in organs except the midgut.

## CHAPTER 3

# The development of *Babesia ovata* in the midgut of *Haemaphysalis longicornis*

**This work has been published as:**

Maeda, H., Hatta, T., Alim, M.A., Tsubokawa, D., Mikami, F., Matsubayashi, M., Umemiya-Shirafuji, R., Tsuji, N., Tanaka, T. (2017). Initial development of *Babesia ovata* in the tick midgut, *Vet. Parasitol.*, ***233***, 39-42.

## 3.1 Introduction

*Babesia* species are tick-borne apicomplexan protozoa that cause babesiosis and affect a wide range of wild and economically important domestic animals as well as humans. *Babesia* organisms show drastic morphological changes in tick tissue when they are transferred from the erythrocytic stages of vertebrate hosts [6, 92, 93]. Since the first discovery and detailed drawings of *Babesia* development in the tick midgut [94, 95], several studies on the midgut form of *Babesia* species have been reported [87, 90, 96, 97]. *B. ovata*, transmitted by the *H. longicornis* tick vector, is a less pathogenic cattle *Babesia* sp. compared to other virulent *Babesia* spp. such as *B. bovis* and *B. bigemina*. However, concomitant infection in cattle with *B. ovata* and *Theileria orientalis* is known to cause an induction of clinical anemia [98]. The *B. ovata* species has recently become a focus of clinical and molecular biological research. The transgenic *B. ovata* is also available as a tool for studying the tick stage of *Babesia* [91]. Higuchi et al. [89, 90, 99–101] worked extensively on the development of *B. ovata* in *H. longicornis* ticks dropped from experimentally *B. ovata*–infected cattle. They reported the development of *B. ovata* in the midgut, salivary glands, and hemolymph of the nymphal tick and also in the ovary and eggs of the adult. However, study on the tick stage of *B. ovata* in the adult tick has

notprogressed, and our knowledge of the entire lifecycle of *B. ovata* from morphological study is insufficient. In this Chapter, I have focused on the initial developmental stages of *B. ovata* in the adult tick midgut by a comparative study from the *in vitro* culture system and *in vivo* study using an artificial feeding system for *H. longicornis* [74].

## 3.2 Materials and methods

### *3.2.1 Ticks and Babesia*

*B. ovata* (Miyake strain) and *H. longicornis* (Okayama strain) [102] maintained at the Department of Parasitology, Kitasato University School of Medicine, were used in this study, and all data were produced from three separate trials.

### *3.2.2 in vitro induction of the development of B. ovata by tick midgut extract*

For the detailed time-course observation, the *in vitro* culture study was conducted as described in the previous report for *B. bigemina* with a slight modification [87]. Briefly, five female adult ticks were artificially engorged with adult bovine serum (Biological Industries Ltd., Cromwell, CT, USA) and bovine erythrocytes (Nippon Bio-Test Laboratories Inc.) purified by removing the leukocyte using a LeukoCatch II filter

(WATSON CO. Ltd., Kobe, Japan) [74]. Ticks were dissected after they engorged, and the midgut was obtained from each tick. The contents from all of the midguts were obtained in the insect Ringer's solution [103] by using forceps, small knives, and pipettes. The cell debris from the contents was removed by centrifuging at 500 *g* for 2 min. The extracted midgut contents were mixed with *B. ovata*–infected erythrocytes having approximately 1% parasitemia and incubated at 25°C. The control was prepared with the insect Ringer's solution and infected erythrocytes. The samples were smeared and stained with Giemsa stain at the indicated time points, as described below, and examined under the light microscope.

### *3.2.3 in vivo observation of the development of B. ovata in the artificially B. ovata-infected ticks*

The development of *B. ovata* was also observed in the tick midgut into which *B. ovata* was inoculated to *H. longicornis* by using an artificial feeding system consisting of *B. ovata*–infected erythrocytes (approximately 1% parasitemia) and adult bovine serum [74]. Artificially engorged ticks were dissected at 12 h post engorgement to obtain the midgut, and contents of midgut were smeared on the slides and stained with Giemsa. IFAT was also performed as described in Chapter 2, with smears of the midgut contents

targeting the *B. ovata* P29 protein [102] homologous to *B. gibsoni* P29 [81], which is localized on the cytoskeleton. The specific fluorescence was detected under a confocal microscope (LSM710; Carl Zeiss).

## 3.3 Results

### *3.3.1 in vitro induction of tick stages of B. ovata development*

The induction of *B. ovata* development was initiated by adding the tick midgut extract from artificially engorged ticks. I observed four sequential phases of *in vitro* development over a time of period of approximately 24 h. The appeared morphological changes were listed as below:

**Phase 1, 1-3 h:**

- The budding paired pyriform merozoites (Fig. 3.1A, panel 1; 2–4 μm in length)
- An interesting form with a thin, string-like cytoplasm (Fig. 3.1A, panel 2; 4–5 μm in length).
- The spherical forms with two nuclei (Fig. 3.1A, panel 3; 4–5 μm in diameter)

**Phase 2, 4-6 h:**

・The leaf-shaped cells with single nuclei (Fig. 3.1A, panel 4; 2–3 μm in diameter)

・The typical aggregation forms (Fig. 3.1A, panels 5, 6; 4–12 μm in diameter)

**Phase 3, 7-9 h:**

・The spiky parasites with one or two nuclei (Fig. 3.1A, panels 7, 8; 3–6 μm in range)

・A large, round parasites with multiple nuclei (Fig. 3.1A, panel 9; 4–9 μm in diameter)

**Phase 4, 10-12 h:**

・The spiky parasites with clear cytoplasm and shorter spikes (Fig. 3.1A, panels 10, 11; 2–5 μm in diameter) than the forms observed in the previous phase.

・The vermicular forms (Fig. 3.1A, panel 12; 4–5 μm in length).

No further development was observed from continuous observation up to 24 h. In the control group, which contained only insect Ringer's solution and *B. ovata*–infected erythrocytes, no morphological change of *B. ovata* merozoites was observed (Fig. 3.1B).

*3.3.2 B. ovata development in ticks*

I found parasites of a shape similar to those observed in the *in vitro* assay, including aggregation forms (Fig. 3.2A, panels 1, 2; Fig. 3.2B, panel 1); spiky parasites

(Fig. 3.2A, panels 4, 5; Fig. 3.2B, panels 4–6); large, round parasites (Fig. 3.2A, panel 3; Fig. 3.2B, panels 2, 3); and vermicular forms (Fig. 3.2A, panel 6). The antibody for the *B. ovata* P29 protein reacted strongly with their cytoskeleton, confirming that their varied morphologies were for *B. ovata* itself. These results indicate that the development of *B. ovata* occurred rapidly and sequentially in the midgut of *H. longicornis* ticks.

## 3.4 Discussion

As shown in Fig. 3.1A, after 1–3 h of incubation, spherical forms with two nuclei (Fig. 3.1A, panel 3) were observed, which were considered to have developed from some of the budding paired pyriform merozoites (Fig. 3.1A, panel 1). I also observed an interesting form with a thin, string-like cytoplasm (Fig. 3.1A, panel 2). This form might be the transition stage from pyriform to spherical form. Then leaf-shaped cells with single nuclei (Fig. 3.1A, panel 4) considered to be the cellular division of spherical forms appeared, and typical aggregation forms (Fig. 3.1A, panels 5, 6) were confirmed at 4–6 h post incubation. Following the appearance of aggregation forms (7–9 h post incubation), spiky parasites with one or two nuclei (Fig. 3.1A, panels 7, 8) were observed. This form was considered to be the ray body (called strahlenkörper by Koch), the sexual stages of

parasites as described in other *Babesia* species [6, 92, 93]. In *B. bigemina*, aggregation forms were observed after the appearance of ray bodies, and this was considered to be their strategy for contact between individual ray bodies [87]. In case of *B. ovata*, the ray bodies were first observed after the appearance of the aggregation form, and it seemed that this aggregation form was an important stage in the transformation to ray bodies. Interestingly, large, round parasites with multiple nuclei (Fig. 3.1A, panel 9) appeared in this phase. This might be a unique, fused form of ray bodies to contact others, as happens in the case of other species of *Babesia* parasites. Higuchi et al. [90] described that in *B. ovata*, there were development of bizarre form protozoa and elongated-form protozoa, considered to be the macrogamete and microgamete, respectively, which fused to produce round-formed protozoa as zygotes. However, in this observation, round protozoa contained multiple nuclei; therefore, this form might be the division form of zygotes for producing the mature ray bodies. At 10–12 h post incubation, the spiky parasites with clear cytoplasm and shorter spikes (Fig. 3.1A, panels 10, 11) than the forms observed in the previous phase appeared. They contained one or two nuclei, and the parasites with a single nucleus might be the mature ray bodies (Fig. 3.1A, panel 11). The ray bodies with two nuclei might be the dividing stage in the development of vermicular forms (Fig. 3.1A, panel 12). No further development was observed from continuous observation up to 24 h.

These results clearly indicated that some factors in midgut contents stimulate the onset of the transformation of *B. ovata* parasites, which is completed within 12 h after incubation. This is relatively slower than the *B. bigemina* development in the midgut of their vector tick, *Rhipicephalus microplus* [87]. Furthermore, Higuchi et al. [90] observed *B. ovata* development in the midgut of the nymphal tick of *H. longicornis*, and they mentioned that the morphological changes were finished at 10 days post engorgement. From these findings and the previous reports, it is obvious that the transition of *Babesia* parasites is faster in adults than in nymphal ticks. The shorter time requirement for development in adult ticks can be related to the transovarial transmission. The factors in the tick midgut that initiate and regulate the development of *B. ovata* are not well understood. To consider the trigger for development of *Plasmodium* parasites in mosquitoes, it was suggested that a mosquito-derived molecule, xanthurenic acid, a temperature shift, or a pH change might be related [104]. Moreover, it was reported that the sexual stages of *B. bigemina* were induced *in vitro* by xanthurenic acid without tick contents [105]. It is considered that the xanthurenic acid of ticks might be one of the key factors in the development of *Babesia* parasites in ticks. Further study is needed to clarify the factor in the tick midgut contents that triggers babesial development. To confirm these morphological changes were surely occurred in the tick midgut, *in vivo* observation using *B. ovata*-infested ticks artificially.

As shown in Fig. 3.2, I found parasites of a shape similar to those observed in the *in vitro* assay, these results indicate that the development of *B. ovata* occurred rapidly and sequentially in the midgut of *H. longicornis* ticks.

In summary, a diagram of the development of *B. ovata* in the tick midgut is shown in Fig.3.3. I observed the initial development of *B. ovata* in the tick midgut, and the morphological changes might be completed within 12 h after tick engorgement. From this observation, it is considered that merozoites (Fig. 3.3a), after taken up by the ticks during blood feeding, develop into two populations of ray bodies (Fig. 3.3g), macrogametes and microgametes, in the midgut environment of the tick. To generate these ray bodies, it seems necessary to form multinucleated aggregation bodies (Fig. 3.3e, f). The single-nucleated ray bodies are assumed to be gametes, and they fuse together in pairs to form diploid zygotes. The zygotes seem to undergo further division for large, round forms (Fig. 3.3h), it may produce the mature ray bodies (Fig. 3.3j) to emerge as haploid vermicular forms (Fig. 3.3k), which might be develop into kinetes. The kinetes will migrate to organs in the hemocoel, including the ovaries of female adult ticks, where further divisions will occur and tick eggs will become pathogenic. In this study, I found novel forms of *B. ovata*: the aggregation forms and the ray bodies with short spikes and clear cytoplasm (Fig. 3.4). Their significance is unknown, but these bodies might play

key roles in generating mature kinetes, which migrate to the hemocoel of ticks. It remains unclear whether these stages are specific in the adult ticks, and different stages from other *Babesia* species. To clarify the relationship between *Babesia* spp. and tick at the midgut level, these findings presented in Chapter 3 will be useful basic knowledge for further study on the tick vector biology.

## Figures in CHAPTER 3

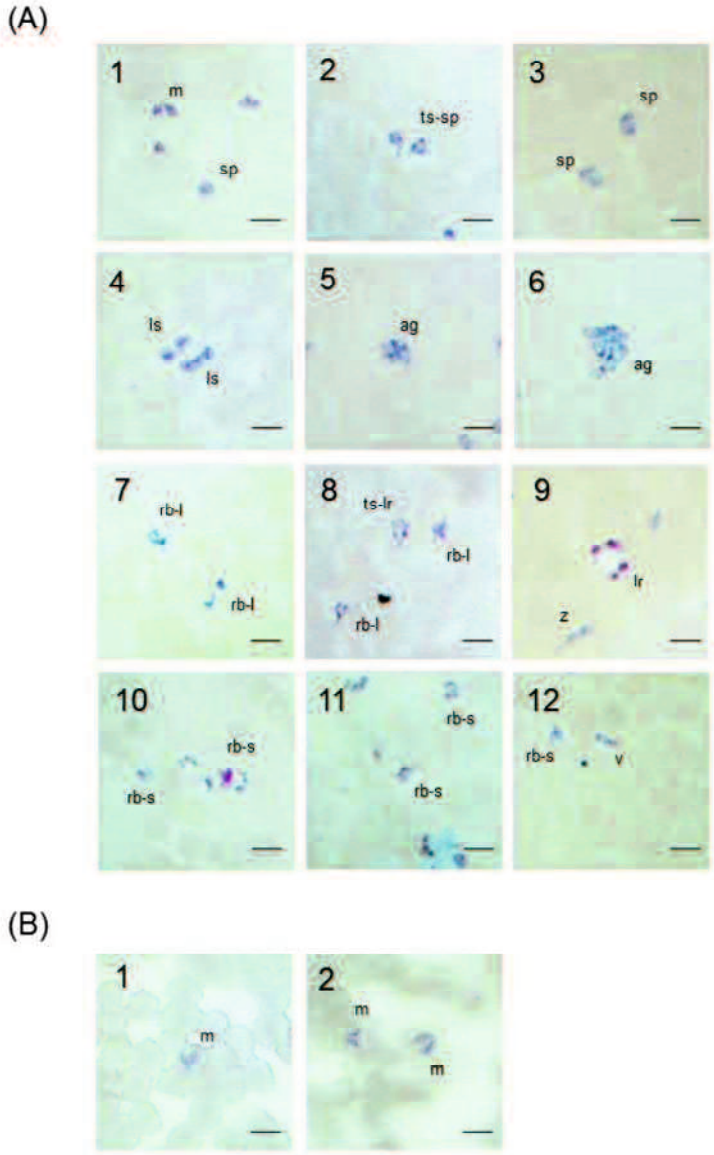


Fig. 3.1 Sequential development of *B. ovata* induced by the tick midgut contents. (A) Development induced group. Representative forms observed in *in vitro* study. Panels 1–3, 1–3 h post incubation (hpi); panels 4–6, 4–6 hpi; panels 7–9, 7–9 hpi; panels 10–12, 10–12 hpi. (B) Control group with no midgut contents: m, merozoites before development; ts-sp, a transition stage from pyriform to spherical form; sp, spherical form; ls, leaf-shaped body; ag, aggregation form; rb-l, ray bodies with long spikes; ts-lr, a transition stage from zygote to large, round form; z, zygote; lr, large, round form; rb-s, ray bodies with short spikes and clear cytoplasm; v, vermicular form. Bar: 5 μm.

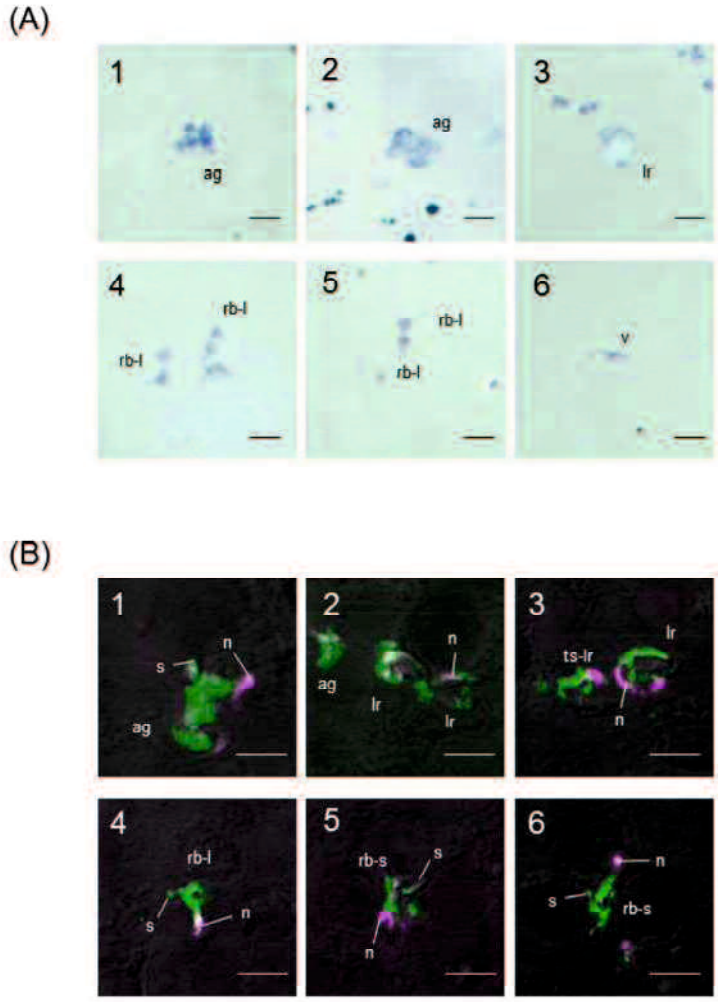


Fig. 3.2 Morphological changes of *B. ovata* parasites in the tick midgut 12 h post engorgement. (A) Giemsa staining. Panels 1, 2, aggregation forms; panel 3, large, round parasites; panels 4, 5, ray bodies; panel 6, vermicular form parasite. (B) Indirect immunofluorescent antibody test. Panel 1, aggregation forms; panels 3, 4, large, round parasites; panels 4–6, ray bodies. n, nucleus; s, spike; ag, aggregation form; rb-l, ray bodies with long spikes; ts-lr, a transition stage from zygote to large, round form; lr, large, round form; rb-s, ray bodies with short spikes and clear cytoplasm; v, vermicular form. Bar: 5 μm.

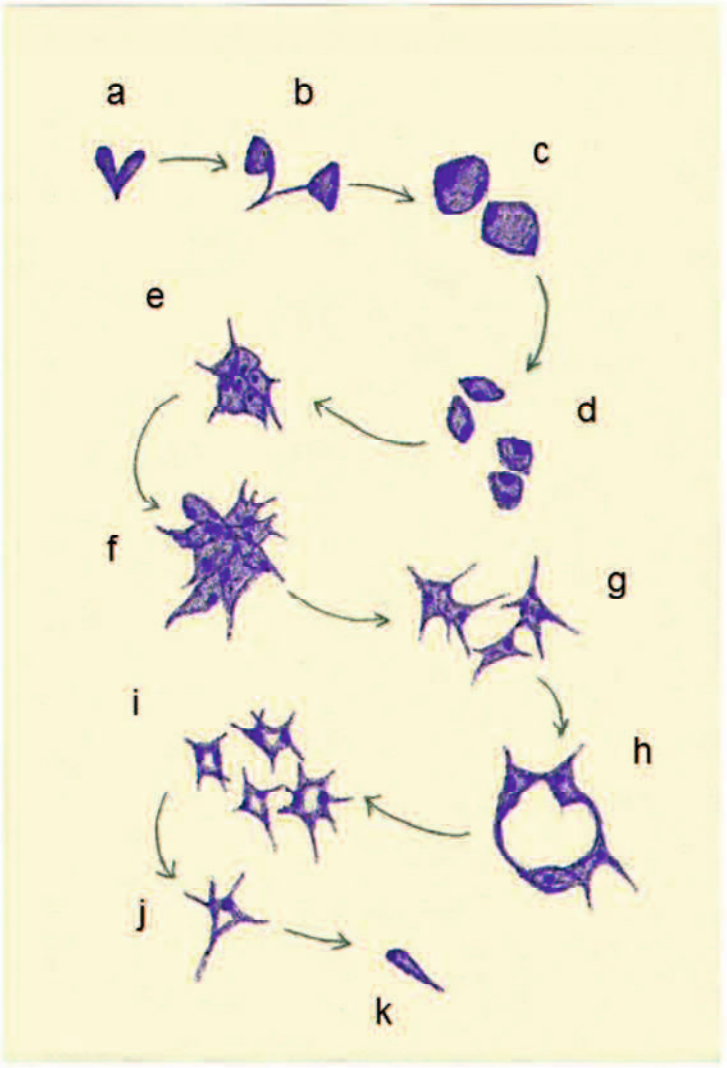


Fig. 3.3 A diagram of the development of *B. ovata* in the tick midgut. (a) Merozoite; (b) transitional form for spherical body; (c) spherical body; (d) leaf-shaped parasites; (e) small aggregation form; (f) large aggregation form; (g) ray bodies; (h) large, round parasite; (i) mature ray bodies (diploid); (j) mature ray bodies (haploid); (k) vermicular form.

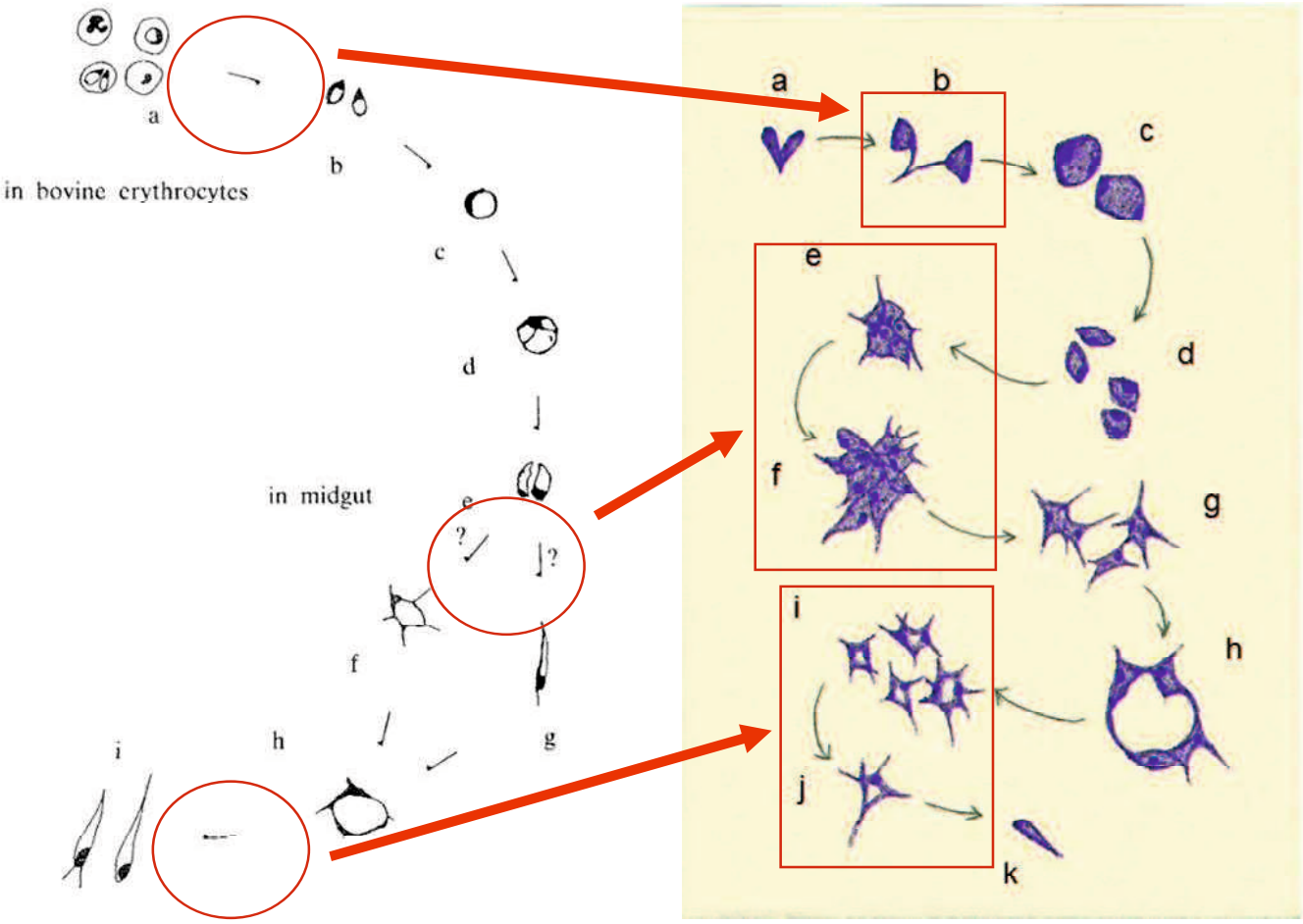


(Higuchi et al., 1989)

Fig. 3.4 A comparative diagram showing the novel findings of the *B. ovata* development in the tick midgut. The left diagram is from the previous research by Dr. Higuchi. The right diagram is from the results in Chapter 3 of this dissertation.

# CHAPTER 4

## The relationship of *Haemaphysalis longicornis* C-type lectin with *Babesia ovata*

## 4.1 Introduction

The two major families of PRRs involve the innate immune system are TLRs and CLec recepters. They are known to relate defense mechanisms against many pathogens including bacteria, viruses, fungi, and helminths [31, 32, 106]. Recently, some CLecs are studied and reported on their relationship with protozoan parasites including *Leishmania*, *Toxoplasma*, and malaria parasites [107–109]. Thus, it is considered that CLecs work with broad recognition spectrum.

In Chapter 1, I identified and characterized novel CLec from *H. longicornis*. I described its important roles in the defense mechanisms against Gram-negative bacteria. In *HlCLec*-silenced ticks, the resistance against *E. coli* were clearly decreased. In Chapter 2 and 3, I established a novel Tick-*Babesia* experimental infection model [102]. The findings suggested that *Babesia* parasites pass through tick midgut within 24 h and migrate to other organs for further multiplication. In the tick midgut, the morphological changes of *Babesia* parasites were also observed. Taken altogether, in this Chapter, I attempt to demonstrate whether HlCLec is relate with the migration of *Babesia* parasites in the ticks.

## 4.2 Materials and Methods

### *4.2.1 Ticks, mice and Babesia*

*H. longicornis* ticks and BALB/c mice were cared in accordance of the guideline of Kitasato University as shown in Chapter 2. *Babesia* parasites (*B. ovata* Miyake strain) [75] were also maintained as shown in Chapter 2 and 3.

### *4.2.2 RNA interference and tick artificial feeding*

RNAi was conducted by injecting 2 μg of *dsHlCLec* or *dsLuc* as shown in Chapter 1. Ticks were artificially infected with *B. ovata* as described in Chapter 2. The ticks were fed on the solution composed of the flesh media and *B. ovata*-infected RBC (Approximately 1~2 % parasitemia). After 0 or 4 DPE, ticks were dissected and separated to midgut, ovary, and carcass.

### *4.2.3 PCR detection of B. ovata DNA in the ticks*

The DNA extraction were performed as described previously [76]. PCR detection of *B. ovata* targeting *B. ovata* β-tubulin fragment was performed as mentioned in Chapter 2. Briefly, PCR detection were conducted with KOD-Plus-Neo enzyme (Toyobo). The cycling conditions were as follows: initial denaturation at 95°C for 2 min,

followed by 40 cycles of denaturation at 98°C for 10 sec, annealing at 60°C for 30 sec, extension at 68°C for 15 sec, and final extension at 68°C for 7 min.

## 4.3 Result

### *4.3.1 The affection of HlClec knockdown to B. ovata infection*

The conventional PCR results in Fig. 4.1 show the existence of *B. ovata β-tubulin* DNA in the tick organs of 4 DPE. In the control group, the bands of *B. ovata* in the midgut samples completely disappear on 4 DPE. On the contrary, those in the ovary and carcass were become positive on 4 DPE. This results was representable as shown in Chapter 2. In Chapter 2, the positive bands of *B. ovata* gradually disappear in the midgut samples, and conversely, those were likely to increase in the ovary and carcass samples after 1 DPE. After *HlCLec* silencing, the tendency are reversed. Despite it was after 4 DPE, the DNA of *B. ovata* were still detected in the midgut samples, and on the contrary, those were not appeared in the ovary and carcass samples.

## 4.4 Discussion

In Chapter 2, it was clearly shown that the after 4 DPE, *B. ovata* parasites in the tick midgut were already pass through the midgut barrier and infected to other

organs. So, I hypothesized if HlCLec are involved Babesial migration in tick body, 4 DPE is the best timing for accent the differences after gene silencing. As hypothesized, it was obviously shown that after *HlCLec* silencing, the DNA of *B. ovata* were still detected in the midgut. On the contrary, in ovary and carcass, it was hard to detect parasite DNA. It seems that HlCLec relates *B. ovata* transmission of tick midgut are blocked by the expressed HlClec in the midgut. *B. ovata* might use tick molecules for their efficient transmission. It might be because of their recognition activity of *B. ovata* related their carbohydrate structure. This is the first report that suggested the involvement with tick Clec and Babesial migration.

In also research field of malaria, numerous studies are focused on the role of TLRs in immunity against malaria, however, the studies on relevance of CLec receptors and malaria parasites are insufficient. Maglinao et al. [109] provided evidences showing the crucial roles of a specific CLec expressed in dendritic cells in malaria-associated pathology. It possible CLecs might have a potential role in innate immunity against protozoan parasites.

Interestingly, for arthropod-borne microbes, there are some reports indicating that the interaction of vector ligands with pathogens relate on the successful acquisition of the microbe from the vertebrate host. The *I. scapularis* tick gut receptor, TROSPA, is

required for spirochetal colonization of *I. scapularis* [110]. The *Aedes aegypti* mosquito CLec, mosGCTL-1, has a critical role for West Nile Virus infection of mosquitos [111]. These reports imply that pathogens have strategies to infect their potential vectors.

Further research will be needed to clarify their important roles relates on protozoan parasites and lead the key design for the establishment of novel drugs or development of a transmission-blocking vaccine.

## Figure in CHAPTER 4

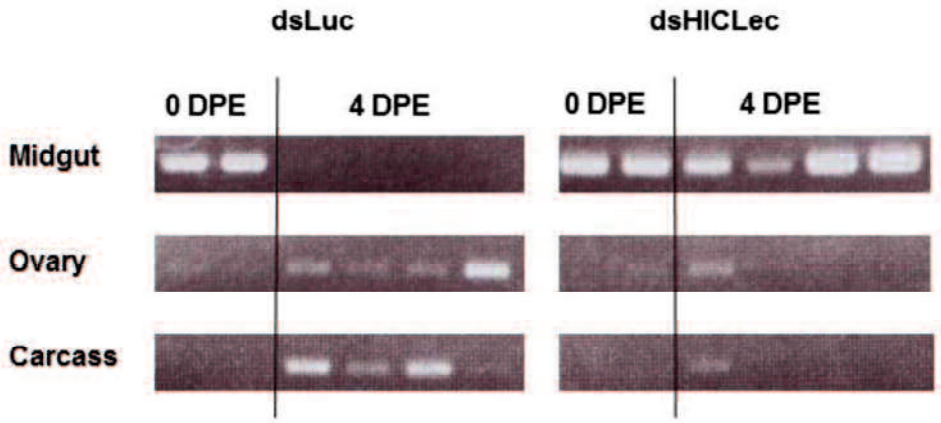


Fig. 4.1. The comparative figure of *B. ovata* migration in ticks after *HlCLec* silencing. The left panel shows the control group. The right panel shows the *HlClec* knockdowned group. DPE: days post engorgement

# SUMMARY AND CONCLUSION

In the defense against infections by host innate immunity, pathogen recognition plays an important role. Pathogens express several evolutionarily conserved signature molecules known as PAMPs, which can be recognized by host sensors such as PRRs [29, 30]. Besides, the most famous PRRs are TLRs, CLec comprise a large receptor superfamily [106, 112]. In ticks, specific protein-carbohydrate interaction is considered to be one of the keys to understand self/non-self recognition and how the transmitted pathogens evade tick immune responses [23, 24]. This dissertation presents my studies on the novel C-type lectin (HlCLec) and its relationship with the migration of *B. ovata*.

In Chapter 1, I conducted the identification and characterization of CLec from *H. longicornis*. HlCLec contains three CRDs, and recombinant proteins show direct binding activity to bacteria. Furthermore, *E. coli* injection after silencing of *HlCLec* gene caused significant decrease in tick survival rate. These data suggest HlCLec has a key role in the innate immunity of ticks against gram-negative bacteria.

It is known that CLecs from some invertebrates are involved with the anti-protozoan parasites [107, 108]. It is also shown that some protozoan might use host CLecs for their migration or transmission [109]. So, I hypothesized that HlCLec might be relate with the migration of *Babesia* parasites. However, compared with mosquito-malaria

relationship, our knowledge of the migration of *B. ovata* in *H. longicornis* is still insufficient. Thus, in Chapter 2, I demonstrated the *B. ovata* migrasion in *H. longicornis* by using an established novel tick-*Babesia* experimentally infection model [102]. This model are based on the artificial feeding system of *H. longicornis* [74]. After that, we could obtain synchronous engorged ticks easily. With the high sensitivity methods of qPCR and IFAT, I concluded that *B. ovata* pass the tick midgut barrier within 24 h after tick engorgement and migrated tick organs including ovary and eggs. In Chapter 3, I detailed described the development of *B. ovata* in the tick midgut. The sequential development of *B. ovata* was confirmed using an artificial induction by tick midgut extract. The results of *in vitro* experiment were representable to *in vivo* experiment from using artificially *B. ovata*-infected ticks.

Finally in Chapter 4, I demonstrated the effect on the gene silencing of *HlCLec* to *B. ovata* migration. After *HlCLec* silencing, the migration of *B. ovata* are clearly changed. Normally, as shown in Chapter 2, *B. ovata* pass through tick midgut within 24 h. However, in the midgut of *HlCLec*-silenced ticks, *B. ovata* DNA was still detectable at 4 DPE. The result indicate that the HlCLec might be one of the key molecule to relate with the infection of *B. ovata* to tick vector.

Taken altogether, the results in this dissertation indicate that CLec of *H.*

*longicornis* involve in the defense mechanism of Gram-negative bacteria and in the passage of *Babesia* parasites in the tick midgut. These evidences obtained from novel methods shown in this dissertation will give us insight toward the novel findings relates with molecules of tick and pathogens, furthermore, for the development of new control strategies of tick transmitted pathogens.

# ACKNOWLEDGEMENT

It is my immense pleasure to express my profound regards and deepest sense of gratitude to my honorable supervisor, Associate Professor Dr. Tetsuya Tanaka (Laboratory of Infectious Diseases, Kagoshima University), for kindly providing me the opportunity of higher study. I gratefully acknowledge his scholastic supervision, invaluable instructions and constructive criticism during my doctoral course.

It gives me great pleasure to express highly appreciations and heartfelt sense of gratitude to my supervisors in the outside institutes, Assistant Professor Dr. Takeshi Hatta and Professor Dr. Naotoshi Tsuji (Laboratory of Parasitology, Kitasato University School of Medicine), for their excellent and continuous supervision to my study, encouragement, and understanding throughout my stay in National Institute of Animal Health (NIAH), and Kitasato University School of Medicine.

My highly appreciations and heartfelt sense of gratitude are extended to my co-supervisors, Professor Dr. Masami Mochizuki (Nippon Veterinary and Life Science University), Associate Professor Dr. Tomohide Matsuo (Laboratory of Parasitology, Kagoshima University), Professor Dr. Hiroshi Sato (Laboratory of Veterinary Parasitology, Yamaguchi University), Professor Dr. Yasuyuki Endo (Laboratory of Small Animal Internal Medicine, Kagoshima University), and Professor Dr. Akikazu Fujita

(Laboratory of Molecular Pathology, Kagoshima University) for accepting me as a PhD student under their supervision and their great patience during reviewing my dissertation critically.

Special thanks to Professor Dr. Kozo Fujisaki (National Research Center for Protozoan Diseases: NRCPD), Assistant Professor Dr. Rika Umemiya-Shirafuji (NRCPD), Assistant Professor Dr. Daigo Tsubokawa (Laboratory of Parasitology, Kitasato University School of Medicine), and Assistant Professor Dr. Remil Linggatong Galay (University of the Philippines Los Baños) for their valuable supports and critical suggestions during my study period.

Special thanks are also expressed to two technicians Dr. Kenkichi Imamura (NIAH) and Dr. Fusako Mikami (Laboratory of Parasitology, Kitasato University School of Medicine) for their continuous technical assistant of my study during my stay in NIAH and Kitasato University School of Medicine.

I am grateful to all of my co-authors in my publications for their special suggestion to improve my manuscript: Associate Professor Dr. Takeshi Miyata (Laboratory of Food Chemistry, Kagoshima University), Professor Dr. M Abdul Alim (Bangladesh Agricultural University), Associate Professor Dr. Makoto Matsubayashi (Laboratory of Veterinary International Prevention, Osaka Prefecture University), Dr.

Takeharu Miyoshi (NIAH), Professor Dr. Shin-ichiro Kawazu (NRCPD), and Professor Dr. Ikuo Igarashi (NRCPD).

My heartfelt gratitude are kindly expressed to all the former and present members of Laboratory of Infectious Diseases, Kagoshima University, especially to Dr. Kodai Kusakisako, Dr. Melbourne Rio Talactac, Dr. Emmanuel Pacia Hernandez, and all undergraduate students for their support and nice friendship.

Finally, I am indebted to my family members for their continuous encouragement during my study tenure. I express my heartfelt gratitude to all of them.

Financial support:

My deepest gratitude to the Japan Society for the Promotion of Science (JSPS) who financially supported my graduate study. I would like to express the deepest appreciation to the JSPS Fellowship program and Grants-in-Aid for Scientific Research 'KAKENHI' that provided me the opportunity for the higher study.

# REFERENCES


1. Bowman, A. S., & Nuttall, P. (2008). *Ticks, Biology, Disease and Control*. Cambridge: Cambridge University Press.
2. Sonenshine, D. E., & Roe, R. M. (2013). *Biology of ticks, vol. 2* (Second ed.). New York: Oxford University Press.
3. Estrada-Peña, A., & Estrada Peña, A. (2015). Ticks as vectors: taxonomy, biology and ecology. *Rev. Sci. Tech.*, ***34***, 53–65.
4. Horak, I. G., Camicas, J. L., & Keirans, J. E. (2002). The Argasidae, Ixodidae and Nuttalliellidae (Acari: Ixodida): a world list of valid tick names. *Exp. Appl. Acarol.*, ***28***, 27–54.
5. Nakao, R., Abe, T., Nijhof, A. M., Yamamoto, S., Jongejan, F., Ikemura, T., & Sugimoto, C. (2013). A novel approach, based on BLSOMs (Batch Learning Self-Organizing Maps), to the microbiome analysis of ticks. *ISME J.*, ***7***, 1003–1015.
6. Chauvin, A., Moreau, E., Bonnet, S., Plantard, O., & Malandrin, L. (2009). *Babesia* and its hosts: Adaptation to long-lasting interactions as a way to achieve efficient transmission. *Vet. Res.*, ***40***, 37.
7. Hajdušek, O., Síma, R., Ayllón, N., Jalovecká, M., Perner, J., de la Fuente, J., & Kopáček, P. (2013). Interaction of the tick immune system with transmitted pathogens. *Front. Cell. Infect. Microbiol.*, ***3***, 26.
8. Homer, M. J., Aguilar-Delfin, I., Telford, S. R., Krause, P. J., & Persing, D. H. (2000). Babesiosis. *Clin. Microbiol. Rev.*, ***13***, 451–469.

9. Schnittger, L., Rodriguez, A. E., Florin-Christensen, M., & Morrison, D. A. (2012). *Babesia*: A world emerging. *Infect. Genet. Evol.*, ***12***, 1788–1809.

10. Ristic, M. (1988). *Babesiosis of Domestic Animals and Man*. Boca Raton: CRC Press.

11. Fujisaki, K., Kawazu, S., & Kamio, T. (1994). The taxonomy of the bovine *Theileria* spp. *Trends Parasitol.*, ***10***, 31–33.

12. Tsuji, N., & Fujisaki, K. (2007). Longicin plays a crucial role in inhibiting the transmission of *Babesia* parasites in the vector tick *Haemaphysalis longicornis*. *Future Microbiol.*, ***2***, 575–578.

13. Tsuji, N., Miyoshi, T., Battsetseg, B., Matsuo, T., Xuan, X., & Fujisaki, K. (2008). A cysteine protease is critical for *Babesia* spp. transmission in *Haemaphysalis* ticks. *PLoS Pathog.*, ***4***, e1000062.

14. Iwanaga, S., & Lee, B. L. (2005). Recent advances in the innate immunity of invertebrate animals. *J. Biochem. Mol. Biol.*, ***38***, 128–150.

15. Tsakas, S., & Marmaras, V. (2010). Insect immunity and its signalling: an overview. *Invertebr. Surviv. J.*, ***7***, 228–238.

16. Hancock, R. E. W., Brown, K. L., & Mookherjee, N. (2006). Host defence peptides from invertebrates - emerging antimicrobial strategies. *Immunobiology*, ***211***, 315–322.

17. Silva, L. P. (2004). Antimicrobial Peptides from Animals: Focus on Drug Discovery. *Lett. Drug Des. Discov.*, ***1***, 230–236.

18. Dodd, R. B., & Drickamer, K. (2001). Lectin-like proteins in model organisms: implications for evolution of carbohydrate-binding activity. *Glycobiology*, ***11***, 71–79.

19. Cerenius, L., Lee, B. L., & Söderhäll, K. (2008). The proPO-system: pros and cons for its role in invertebrate immunity. *Trends Immunol.*, ***29***, 263–271.

20. González-Santoyo, I., & Córdoba-Aguilar, A. (2012). Phenoloxidase: A key component of the insect immune system. *Entomol. Exp. Appl.*, ***142***, 1–16.

21. Brehélin, M. (1986). *Immunity in Invertebrates*. Berlin: Springer Berlin Heidelberg.

22. Ottaviani, E. (2005). Insect immunorecognition. *Invertebr. Surviv. J.*, ***2***, 142–151.

23. Söderhäll, K. (2010). *Invertebrate Immunity* (*Advances in Experimental Medicine and Biology*). Springer.

24. Taylor, D. (2006). Innate Immunity in Ticks: A review. *J. Acarol. Soc. Japan*, ***15***, 109–127.

25. Ceraul, S. M., Sonenshine, D. E., & Hynes, W. L. (2002). Resistance of the tick *Dermacentor variabilis* (Acari: Ixodidae) following challenge with the bacterium *Escherichia coli* (Enterobacteriales: Enterobacteriaceae). *J. Med. Entomol.*, ***39***, 376–383.

26. Eggenberger, L. R., Lamoreaux, W. J., & Coons, L. B. (1990). Hemocytic encapsulation of implants in the tick *Dermacentor variabilis*. *Exp. Appl. Acarol.*, ***9***, 279–287.

27. Grubhoffer, L., Kovar, V., & Rudenko, N. (2004). Tick lectins: Structural and functional properties. *Parasitology*, ***129***, 113–125.

28. Grubhoffer, L., & Jindrak, L. (1998). Lectins and tick-pathogen interactions: a minireview. *Folia Parasitol. (Praha).*, ***45***, 9–13.

29. Kumar, H., Kawai, T., & Akira, S. (2011). Pathogen recognition by the innate immune system. *Int. Rev. Immunol.*, ***30***, 16–34.

30. Takeuchi, O., & Akira, S. (2010). Pattern Recognition Receptors and Inflammation. *Cell*, ***140***, 805–820.

31. Cambi, A., Koopman, M., & Figdor, C. G. (2005). How C-type lectins detect pathogens. *Cell. Microbiol.*, ***7***, 481–488.

32. Dambuza, I. M., & Brown, G. D. (2015). C-type lectins in immunity: Recent developments. *Curr. Opin. Immunol.*, ***32***, 21–27.

33. Zelensky, A. N., & Gready, J. E. (2005). The C-type lectin-like domain superfamily. *FEBS J.*, ***272***, 6179–6217.

34. Smith, A. A., & Pal, U. (2014). Immunity-related genes in *Ixodes scapularis*-perspectives from genome information. *Front. Cell. Infect. Microbiol.*, ***4***, 116.

35. Takase, H., Watanabe, A., Yoshizawa, Y., Kitami, M., & Sato, R. (2009). Identification and comparative analysis of three novel C-type lectins from the silkworm with functional implications in pathogen recognition. *Dev. Comp. Immunol.*, ***33***, 789–800.

36. Wang, X. W., & Wang, J. X. (2012). Diversity and multiple functions of lectins in shrimp immunity. *Dev. Comp. Immunol.*, ***39***, 27–38.

37. Zhang, H., Wang, H., Wang, L., Song, L., Song, X., Zhao, J., Li, L., & Qiu, L. (2009). Cflec-4, a multidomain C-type lectin involved in immune defense of Zhikong scallop *Chlamys farreri*. *Dev. Comp. Immunol.*, ***33***, 780–788.

38. Cirimotich, C. M., Dong, Y., Garver, L. S., Sim, S., & Dimopoulos, G. (2010). Mosquito immune defenses against *Plasmodium* infection. *Dev. Comp. Immunol.*, ***34***, 387–395.

39. Fujisaki, K. (1978). Development of acquired resistance precipitating antibody in rabbits experimentally infested with females of *Haemaphysalis longicornis* (Ixodoidea: Ixodidae). *Natl. Inst. Anim. Heal. Q. Tokyo*, ***18***, 27–38.

40. Huang, X., Huang, Y., Shi, Y. R., Ren, Q., & Wang, W. (2015). Function of a novel C-type lectin with two CRD domains from *Macrobrachium rosenbergii* in innate immunity. *Dev. Comp. Immunol.*, ***49***, 121–126.

41. Shi, X. Z., Kang, C. J., Wang, S. J., Zhong, X., Beerntsen, B. T., & Yu, X. Q. (2014). Functions of *Armigeres subalbatus* C-type lectins in innate immunity. *Insect Biochem. Mol. Biol.*, ***52***, 102–114.

42. Efimov, V. P., Lustig, A., & Engel, J. (1994). The thrombospondin-like chains of cartilage oligomeric matrix protein are assembled by a five-stranded α-helical bundle between residues 20 and 83. *FEBS Lett.*, ***341***, 54–58.

43. Miyata, T., Harakuni, T., Tsuboi, T., Sattabongkot, J., Ikehara, A., Tachibana, M., Torii, M., Matsuzaki, G., & Arakawa, T. (2011). Tricomponent immunopotentiating system as a novel molecular design strategy for malaria vaccine development. *Infect. Immun.*, ***79***, 4260–4275.

44. Zhou, J., Liao, M., Ueda, M., Gong, H., Xuan, X., & Fujisaki, K. (2007). Sequence characterization and expression patterns of two defensin-like antimicrobial peptides from the tick *Haemaphysalis longicornis*. *Peptides*, ***28***, 1304–1310.

45. Koizumi, N., Imamura, M., Kadotani, T., Yaoi, K., Iwahana, H., & Sato, R. (1999). The lipopolysaccharide-binding protein participating in hemocyte nodule formation in the silkworm *Bombyx mori* is a novel member of the C-type lectin superfamily with two different tandem carbohydrate-recognition domains. *FEBS Lett.*, ***443***, 139–143.

46. Wang, L., Wang, L., Yang, J., Zhang, H., Huang, M., Kong, P., Zhou, Z., & Song, L. (2012). A multi-CRD C-type lectin with broad recognition spectrum and cellular adhesion from *Argopecten irradians*. *Dev. Comp. Immunol.*, ***36***, 591–601.

47. Hoppe, H. J., & Reid, K. B. (1994). Trimeric C-type lectin domains in host defence. *Structure*, ***2***, 1129–1133.

48. McMahon, S. A., Miller, J. L., Lawton, J. A., Kerkow, D. E., Hodes, A., Marti-Renom, M. A., Doulatov, S., Narayanan, E., Sali, A., Miller, J. F., & Ghosh, P. (2005). The C-type lectin fold as an evolutionary solution for massive sequence variation. *Nat. Struct. Mol. Biol.*, ***12***, 886–892.

49. Liu, X. Y., & Bonnet, S. I. (2014). Hard Tick Factors Implicated in Pathogen Transmission. *PLoS Negl. Trop. Dis.*, ***8***, e2566.

50. McGreal, E. P., Miller, J. L., & Gordon, S. (2005). Ligand recognition by antigen-presenting cell C-type lectin receptors. *Curr. Opin. Immunol.*, ***17***, 18–24.

51. de Pedro, M. A., & Cava, F. (2015). Structural constraints and dynamics of bacterial cell wall architecture. *Front. Microbiol.*, ***6***, 1–10.

52. Münch, D., & Sahl, H. G. (2015). Structural variations of the cell wall precursor lipid II in Gram-positive bacteria - Impact on binding and efficacy of antimicrobial peptides. *Biochim. Biophys. Acta - Biomembr.*, ***1848***, 3062–3071.

53. Smith, C. A. (2006). Structure, Function and Dynamics in the mur Family of Bacterial Cell Wall Ligases. *J. Mol. Biol.*, ***362***, 640–655.

54. Mukherjee, S., Zheng, H., Derebe, M. G., Callenberg, K. M., Partch, C. L., Rollins, D., Propheter, D. C., Rizo, J., Grabe, M., Jiang, Q. X., & Hooper, L. V. (2014). Antibacterial membrane attack by a pore-forming intestinal C-type lectin. *Nature*, ***505***, 103–107.

55. Yu, Y., Huang, H., Feng, K., Pan, M., Yuan, S., Huang, S., Wu, T., Guo, L., Dong, M., Chen, S., & Xu, A. (2007). A Short-Form C-Type Lectin from Amphioxus Acts as a Direct Microbial Killing Protein via Interaction with Peptidoglycan and Glucan. *J. Immunol.*, ***179***, 8425–8434.

56. Li, M., Li, C., Ma, C., Li, H., Zuo, H., Weng, S., Chen, X., Zeng, D., He, J., & Xu, X. (2014). Identification of a C-type lectin with antiviral and antibacterial activity from pacific white shrimp *Litopenaeus vannamei*. *Dev. Comp. Immunol.*, ***46***, 231–240.

57. Yang, J., Huang, M., Zhang, H., Wang, L., Wang, H., Wang, L., Qiu, L., & Song, L. (2015). CfLec-3 from scallop: an entrance to non-self recognition mechanism of invertebrate C-type lectin. *Sci. Rep.*, ***5***, 10068.

58. Ohta, M., Kawazu, S., Terada, Y., Kamio, T., Tsuji, M., & Fujisaki, K. (1996). Experimental transmission of *Babesia ovata* oshimensis n. var. of cattle in Japan by *Haemaphysalis longicornis*. *J. Vet. Med. Sci.*, ***58***, 1153–1155.

59. Gayo, V., Romito, M., Nel, L. H., Solari, M. A., & Viljoen, G. J. (2003). PCR-based detection of the transovarial transmission of Uruguayan *Babesia bovis* and *Babesia bigemina* Vaccine Strains. *Onderstepoort. J. Vet. Res.*, ***70***, 197–204.

60. Howell, J. M., Ueti, M. W., Palmer, G. H., Scoles, G. A., & Knowles, D. P. (2007). Persistently infected calves as reservoirs for acquisition and transovarial transmission of *Babesia bovis* by *Rhipicephalus* (*Boophilus*) *microplus*. *J. Clin. Microbiol.*, ***45***, 3155–3159.

61. Howell, J. M., Ueti, M. W., Palmer, G. H., Scoles, G. A., & Knowles, D. P. (2007). Transovarial transmission efficiency of *Babesia bovis* tick stages acquired by *Rhipicephalus* (*Boophilus*) *microplus* during acute infection. *J. Clin. Microbiol.*, ***45***, 426–431.

62. Cohuet, A., Osta, M. A., Morlais, I., Awono-Ambene, P. H., Michel, K., Simard, F., Christophides, G. K., Fontenille, D., & Kafatos, F. C. (2006). *Anopheles* and *Plasmodium*: from laboratory models to natural systems in the field. *EMBO Rep.*, *7*, 1285–1289.

63. Sinden, R. E. (2015). The cell biology of malaria infection of mosquito: Advances and opportunities. *Cell. Microbiol.*, ***17***, 451–466.

64. Beier, J. C. (1998). Malaria parasite development in mosquitoes. *Annu. Rev. Entomol.*, ***43***, 519–43.

65. Ristic, M., & Kreier, J. P. (1981). *Babesiosis*. New York: Academic press.

66. Weinman, D., & Ristic, M. (1968). *Infectious Blood Diseases of Man and Animals, vol. 2.* New York and London: Academic press.

67. Andrade, J. J., Xu, G., & Rich, S. M. (2014). A silicone membrane for *in vitro* feeding of *Ixodes scapularis* (Ixodida: Ixodidae). *J. Med. Entomol.*, ***51***, 878–879.

68. Lew-Tabor, A. E., Bruyeres, A. G., Zhang, B., & Rodriguez Valle, M. (2014). *Rhipicephalus* (*Boophilus*) *microplus* tick *in vitro* feeding methods for functional (dsRNA) and vaccine candidate (antibody) screening. *Ticks. Tick. Borne. Dis.*, ***5***, 500–510.

69. Liu, X. Y., Cote, M., Paul, R. E. L., & Bonnet, S. I. (2014). Impact of feeding system and infection status of the blood meal on *Ixodes ricinus* feeding. *Ticks. Tick. Borne. Dis.*, ***5***, 323–328.

70. Billeter, S. A., Kasten, R. W., Killmaster, L. F., Breitschwerdt, E. B., Levin, M. L., Levy, M. G., Kosoy, M. Y., & Chomel, B. B. (2012). Experimental infection by capillary tube feeding of *Rhipicephalus sanguineus* with *Bartonella vinsonii* subspecies *berkhoffii*. *Comp. Immunol. Microbiol. Infect. Dis.*, ***35***, 9–15.

71. Macaluso, K. R., Sonenshine, D. E., Ceraul, S. M., & Azad, A. F. (2001). Infection and transovarial transmission of rickettsiae in *Dermacentor variabilis* ticks acquired by artificial feeding. *Vector Borne Zoonotic Dis.*, ***1***, 45–53.

72. Oliver, J. D., Lynn, G. E., Burkhardt, N. Y., Price, L. D., Nelson, C. M., Kurtti, T. J., & Munderloh, U. G. (2016). Infection of immature *Ixodes scapularis* (Acari: Ixodidae) by membrane feeding. *J. Med. Entomol.*, ***53***, 409–415.

73. Sonenshine, D. E., & Roe, R. M. (2013). *Biology of ticks, vol. 1* (Second ed.). New York: Oxford University Press.

74. Hatta, T., Miyoshi, T., Matsubayashi, M., Islam, M. K., Alim, M. A., Anisuzzaman, Yamaji, K., Fujisaki, K., & Tsuji, N. (2012). Semi-artificial mouse skin membrane feeding technique for adult tick, *Haemaphysalis longicornis*. *Parasit. Vectors*, ***5***, 263.

75. Igarashi, I., Avarzed, A., Tanaka, T., Inoue, N., Ito, M., Omata, Y., Saito, A., & Suzuki, N. (1994). Continuous *in vitro* cultivation of *Babesia ovata*. *J. Protozool. Res.*, ***4***, 111–118.

76. Maeda, H., Boldbaatar, D., Kusakisako, K., Galay, R. L., Aung, K. M., Umemiya-Shirafuji, R., Mochizuki, M., Fujisaki, K., & Tanaka, T. (2013). Inhibitory effect of cyclophilin A from the hard tick *Haemaphysalis longicornis* on the growth of *Babesia bovis* and *Babesia bigemina*. *Parasitol. Res.*, ***112***, 2207–2213.

77. Sivakumar, T., Tattiyapong, M., Okubo, K., Suganuma, K., Hayashida, K., Igarashi, I., Zakimi, S., Matsumoto, K., Inokuma, H., & Yokoyama, N. (2014). PCR detection of *Babesia ovata* from questing ticks in Japan. *Ticks. Tick. Borne. Dis.*, ***5***, 305–310.

78. Hatta, T., Matsubayashi, M., Miyoshi, T., Islam, M. K., Alim, M. A., Anisuzzaman, Yamaji, K., Fujisaki, K., & Tsuji, N. (2013). Quantitative PCR-based parasite burden estimation of *Babesia gibsoni* in the vector tick, *Haemaphysalis longicornis* (acari: Ixodidae), fed on an experimentally infected dog. *J. Vet. Med. Sci.*, ***75***, 1–6.

79. Anisuzzaman, Hatta, T., Miyoshi, T., Matsubayashi, M., Islam, M. K., Alim, M. A., Anas, M. A., Hasan, M. M., Matsumoto, Y., Yamamoto, Y., Yamamoto, H., Fujisaki, K., & Tsuji, N. (2014). Longistatin in tick saliva blocks advanced glycation end-product receptor activation. *J. Clin. Invest.*, ***124***, 4429–4444.

80. Anderson-White, B. R., Ivey, F. D., Cheng, K., Szatanek, T., Lorestani, A., Beckers, C. J., Ferguson, D. J., Sahoo, N., & Gubbels, M. J. (2011). A family of intermediate filament-like proteins is sequentially assembled into the cytoskeleton of *Toxoplasma gondii*. *Cell. Microbiol.*, ***13***, 18–31.

81. Fukumoto, S., Xuan, X., Inoue, N., Igarashi, I., Sugimoto, C., Fujisaki, K., Nagasawa, H., Mikami, T., & Suzuki, H. (2003). Molecular characterization of a gene encoding a 29-kDa cytoplasmic protein of *Babesia gibsoni* and evaluation of its diagnostic potentiality. *Mol. Biochem. Parasitol.*, ***131***, 129–136.

82. Islam, M. K., Tsuji, N., Miyoshi, T., Alim, M. A., Huang, X., Takeshi, H., & Fujisaki, K. (2009). The Kunitz-like modulatory protein haemangin is vital for hard tick blood-feeding success. *PLoS Pathog.*, ***5***, e1000497.

83. Maeda, H., Kurisu, K., Miyata, T., Kusakisako, K., Galay, R. L., Rio, T. M., Mochizuki, M., Fujisaki, K., & Tanaka, T. (2015). Identification of the *Babesia*-responsive leucine-rich repeat domain-containing protein from the hard tick *Haemaphysalis longicornis*. *Parasitol. Res.*, ***114***, 1793–1802.

84. Dalgliesh, R., & Stewart, N. P. (1977). Failure of vaccine strains of *Babesia bovis* to regain infectivity for ticks during long-standing infections in cattle. *Aust. Vet. J.*, ***53***, 429–431.

85. Stewart, N. P. (1978). Differences in the life cycles between a vaccine strain and an unmodified strain of *Babesia bovis* (Babes, 1889) in the tick *Boophilus microplus* (Canestrini). *J. Protozool.*, ***25***, 497–501.

86. Timms, P., Stewart, N. P., & De Vos, A. J. (1990). Study of virulence and vector transmission of *Babesia bovis* by use of cloned parasite lines. *Infect. Immun.*, ***58***, 2171–2176.

87. Gough, J. M., Jorgensen, W. K., & Kemp, D. H. (1998). Development of tick gut forms of *Babesia bigemina in vitro*. *J Eukaryot Microbiol.*, ***45***, 298–306.

88. Bock, R., Jackson, L., de Vos, A., & Jorgensen, W. (2004). Babesiosis of cattle. *Parasitology.*, ***129***, 247–269.

89. Higuchi, S., Hamana, M., Etoh, K., Kawamura, S., & Yasuda, Y. (1991). Development of *Babesia ovata* in the ovary and eggs of the tick, *Haemaphysalis longicornis*. *Kitasato Arch. Exp. Med.*, ***64***, 133–139.

90. Higuchi, S., Ezura, K., Hamana, M., Kawamura, S., & Yasuda, Y. (1989). Development of *Babesia ovata* in the midgut of the tick, *Haemaphysalis longicornis*. *Nihon Juigaku Zasshi.*, ***51***, 1129–1135.

91. Hakimi, H., Yamagishi, J., Kegawa, Y., Kaneko, O., Kawazu, S., & Asada, M. (2016). Establishment of transient and stable transfection systems for *Babesia ovata*. *Parasit. Vectors*, ***9***, 171.

92. Florin-Christensen, M., & Schnittger, L. (2009). Piroplasmids and ticks: a long-lasting intimate relationship. *Front. Biosci.*, ***14***, 3064–3073.

93. Mehlhorn, H., & Schein, E. (1984). The piroplasms: life cycle and sexual stages. *Adv. Parasitol.*, ***23***, 37–103.

94. Kleine, F. K. (1906). Kultivierungsversuch der Hundepiroplasmen. *Zeitschr. f. Hyg.*, ***54***, 10–16.

95. Koch, R. (1906). Beiträgezur Entwicklungsgeschichte der Piroplasmen. *Zeitschr. f. Hyg.*, ***54***, 1–9.

96. Mehlhorn, H., Schein, E., & Voigt, W. P. (1980). Light and electron microscopic study on developmental stages of *Babesia canis* within the gut of the tick *Dermacentor reticulatus*. *J. Parasitol.*, ***66***, 220–228.

97. Zapf, F., & Schein, E. (1994). The development of *Babesia* (*Theileria*) *equi* (Laveran, 1901) in the gut and the haemolymph of the vector ticks, *Hyalomma* species. *Parasitol. Res.*, ***80***, 297–302.

98. Sivakumar, T., Tagawa, M., Yoshinari, T., Ybañez, A. P., Igarashi, I., Ikehara, Y., Hata, H., Kondo, S., Matsumoto, K., Inokuma, H., & Yokoyama, N. (2012). PCR detection of *Babesia ovata* from cattle reared in Japan and clinical significance of coinfection with *Theileria orientalis*. *J. Clin. Microbiol.*, ***50***, 2111–2113.

99. Higuchi, S., Itoh, N., Kawamura, S., & Yasuda, Y. (1987). Observation on kinetes of *Babesia ovata* in the hemolymph of the vector tick *Haemaphysalis longicornis*. *Nihon Juigaku Zasshi*, ***49***, 1145–1147.

100. Higuchi, S., Oya, H., Hoshi, F., Kawamura, S., & Yasuda, Y. (1994). Development of *Babesia ovata* in the salivary glands of the nymphal tick, *Haemaphysalis longicornis*. *J. Vet. Med. Sci.*, ***56***, 207–209.

101. Higuchi, S., Etoh, K., Nakazato, Y., Kawamura, S., & Yasuda, Y. (1989). Development of *Babesia ovata* in the haemolymph of the tick, *Haemaphysalis longicornis*. *Kitasato Arch. Exp. Med.*, ***62***, 123–127.

102. Maeda, H., Hatta, T., Alim, M. A., Tsubokawa, D., Mikami, F., Matsubayashi, M., Miyoshi, T., Umemiya-Shirafuji, R., Kawazu, S., Igarashi, I., Mochizuki, M., Tsuji, N., & Tanaka, T. (2016). Establishment of a novel tick-*Babesia* experimental infection model. *Sci. Rep.*, ***6***, 37039.

103. Bay, C. M. (1978). The control of enzyme secretion from fly salivary glands. *J. Physiol.*, ***274***, 421–455.

104. Aly, A. S., Vaughan, A. M., & Kappe, S. H. (2009). Malaria Parasite Development in the Mosquito and Infection of the Mammalian Host. *Annu. Rev. Microbiol.*, ***63***, 195–221.

105. Mosqueda, J., Falcon, A., Antonio Alvarez, J., Alberto Ramos, J., Oropeza-Hernandez, L. F., & Figueroa, J. V. (2004). *Babesia bigemina* sexual stages are induced *in vitro* and are specifically recognized by antibodies in the midgut of infected *Boophilus microplus* ticks. *Int. J. Parasitol.*, ***34***, 1229–1236.

106. Drummond, R. A., & Brown, G. D. (2013). Signalling C-Type Lectins in Antimicrobial Immunity. *PLoS Pathog.*, ***9***, 9–11.

107. Castanheira, L., Naves de Souza, D. L., Silva, R. J., Barbosa, B., Mineo, J. R., Tudini, K. A., Rodrigues, R., Ferro, E. V., & de Melo Rodrigues, V. (2015). Insights into anti-parasitism induced by a C-type lectin from *Bothrops pauloensis* venom on *Toxoplasma gondii*. *Int. J. Biol. Macromol.*, ***74***, 568–574.

108. Castanheira, L. E., Nunes, D. C. de O., Cardoso, T. M., Santos, P. de S., Goulart, L. R., Rodrigues, R. S., Richardson, M., Borges, M. H., Yoneyama, K. A. G., & Rodrigues, V. M. (2013). Biochemical and functional characterization of a C-type lectin (BpLec) from *Bothrops pauloensis* snake venom. *Int. J. Biol. Macromol.*, ***54***, 57–64.

109. Maglinao, M., Klopfleisch, R., Seeberger, P. H., & Lepenies, B. (2013). The C-type lectin receptor DCIR is crucial for the development of experimental cerebral malaria. *J. Immunol.*, ***191***, 2551–2559.

110. Pal, U., Li, X., Wang, T., Montgomery, R. R., Ramamoorthi, N., Aravinda, M., Bao, F., Yang, X., Pypaert, M., Pradhan, D., Kantor, F. S., Telford, S., Anderson, J. F., Fikrig, E., Haven, N., Hill, C., & Carolina, N. (2004). TROSPA , an *Ixodes scapularis* Receptor for *Borrelia burgdorferi*. *Cell*, ***119***, 457–468.

111. Cheng, G., Cox, J., Wang, P., Krishnan, M. N., Dai, J., Qian, F., & Anderson, J. F. (2010). A C-Type Lectin Collaborates with a CD45 Phosphatase Homolog to Facilitate West Nile Virus Infection of Mosquitoes. *Cell*, ***142***, 714–725.

112. Hoving, J. C., Wilson, G. J., & Brown, G. D. (2014). Signalling C-type lectin receptors, microbial recognition and immunity. *Cell. Microbiol.*, ***16***, 185–194.

## PUBLICATIONS FROM THIS DISSERTATION

Developmental and Comparative Immunology 57 (2016) 38–47

Contents lists available at ScienceDirect

Developmental and Comparative Immunology

journal homepage: www.elsevier.com/locate/dci

# A novel C-type lectin with triple carbohydrate recognition domains has critical roles for the hard tick *Haemaphysalis longicornis* against Gram-negative bacteria

Hiroki Maeda [a, b], Takeshi Miyata [c], Kodai Kusakisako [a, b], Remil Linggatong Galay [d], Melbourne Rio Talactac [a, b], Rika Umemiya-Shirafuji [e], Masami Mochizuki [a, b], Kozo Fujisaki [f], Tetsuya Tanaka [a, b, *]

[a] Laboratory of Infectious Diseases, Joint Faculty of Veterinary Medicine, Kagoshima University, Korimoto, Kagoshima 890-0065, Japan
[b] Department of Pathological and Preventive Veterinary Science, The United Graduate School of Veterinary Science, Yamaguchi University, Yoshida, Yamaguchi 753-8515, Japan
[c] Division of Molecular Functions of Food, Department of Biochemistry and Biotechnology, Kagoshima University, Korimoto, Kagoshima 890-0065, Japan
[d] Department of Veterinary Paraclinical Sciences, College of Veterinary Medicine, University of the Philippines Los Baños, Los Baños, Laguna 4031, Philippines
[e] National Research Center for Protozoan Diseases, Obihiro University of Agriculture and Veterinary Medicine, Inada, Obihiro, Hokkaido 080-8555, Japan
[f] Zen-noh Institute of Animal Health, Ooja, Sakura, Chiba 285-0043, Japan

ARTICLE INFO

*Article history:*
Received 27 August 2015
Received in revised form
17 December 2015
Accepted 17 December 2015
Available online 25 December 2015

*Keywords:*
Tick
C-type lectin
Innate immunity
Recombinant
Gram-negative bacteria

ABSTRACT

C-type lectins (CLecs) play an important role in innate immunity against invaders. In this study, a novel CLec was identified from *Haemaphysalis longicornis* ticks (HlCLec). HlCLec contains a signal peptide and a transmembrane region. Interestingly, HlCLec possesses three dissimilar carbohydrate recognition domains (CRDs). Each CRD contains the mutated motif of $Ca^{2+}$-binding site 2. *HlCLec* mRNA was up-regulated during blood feeding, and had highest expression in the midgut and ovary. HlCLec localization was also confirmed by immunofluorescent antibody test (IFAT). HlCLec was found on the cell membrane and basal lamina of midgut and ovary. In addition, the recombinant HlCLec and individual CRDs demonstrated direct binding activity to *Escherichia coli* and *Staphylococcus aureus*; however, no growth inhibition activity was observed. Furthermore, *E. coli* injection after silencing of *HlCLec* caused drastic reduction in survival rate of ticks. These results strongly suggest the key role of HlCLec in tick innate immunity against Gram-negative bacteria.



## 1. Introduction

The innate immune system is the first line of host defense for sensing invading pathogens by recognition of their specific structural components (pathogen-associated molecular patterns: PAMPs) through pattern recognition receptors (PRRs). Currently, some PRRs including Toll-like receptor (TLR) have been already identified and classified (Kumar et al., 2011; Takeuchi and Akira, 2010). C-type lectin (CLec) is also known as one of the PRRs playing important roles in non-self clearance of pathogens (Cambi et al., 2005; Dambuza and Brown, 2015). CLec consists a large family containing at least one carbohydrate recognition domain (CRD), which share a common structure, such as the EPN motif and QPD motif for the carbohydrate recognition. Although CLec also recognize non-carbohydrate matters, the mechanisms are not fully understood (Zelensky and Gready, 2005).

Ticks are capable of transmitting a wide variety of pathogens, and are ranked second only to mosquitoes as vectors. Even though their vector competence is considered closely involved to their immune system, the detailed knowledge of tick innate immunity is insufficient (Hajdušek et al., 2013; Kopáček et al., 2010; Taylor, 2006). The lectin of ticks have not received the same attention level as those of other species (Grubhoffer et al., 2004). Papers on tick lectins that have been published were very few, and more research data are needed to complete our knowledge for the role of

* Corresponding author. Laboratory of Infectious Diseases, Joint Faculty of Veterinary Medicine, Kagoshima University, 1-21-24 Korimoto, Kagoshima 890-0065, Japan.
*E-mail address:* tetsuya@ms.kagoshima-u.ac.jp (T. Tanaka).

http://dx.doi.org/10.1016/j.dci.2015.12.015
0145-305X/

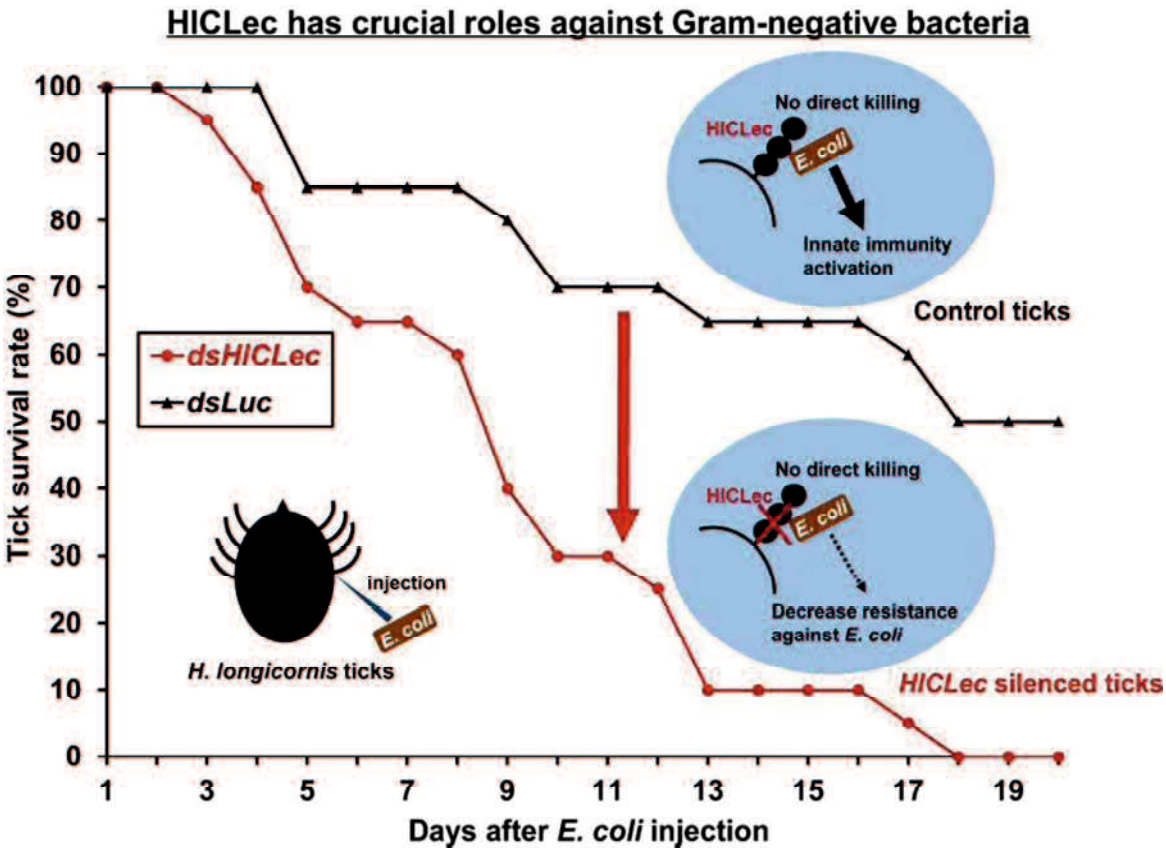


**Graphical abstract from:**

Maeda, H., Miyata, T., Kusakisako, K., Galay, R.L., Talactac, M.R., Umemiya-Shirafuji, R., Mochizuki, M., Fujisaki, K. & Tanaka, T. (2016). A novel C-type lectin with triple carbohydrate recognition domains has critical roles for the hard tick *Haemaphysalis longicornis* against Gram-negative bacteria. *Dev. Comp. Immunol.*, ***57***, 38-47.

SCIENTIFIC REPORTS

OPEN

# Establishment of a novel tick-*Babesia* experimental infection model

Received: 01 June 2016
Accepted: 24 October 2016
Published: 14 November 2016

Hiroki Maeda[1,2], Takeshi Hatta[3], M Abdul Alim[4,5], Daigo Tsubokawa[3], Fusako Mikami[3], Makoto Matsubayashi[6], Takeharu Miyoshi[5], Rika Umemiya-Shirafuji[7], Shin-ichiro Kawazu[7], Ikuo Igarashi[7], Masami Mochizuki[1,2], Naotoshi Tsuji[3] & Tetsuya Tanaka[1,2]

**Ticks are potent vectors of many deadly human and animal pathogens. Tick-borne babesiosis is a well-recognized malaria-like disease that occurs worldwide and recently has attracted increased attention as an emerging zoonosis. Although the proliferation of *Babesia* organisms is essential in the vectors, their detailed lifecycle with time information for migration in ticks remains unknown. A novel study model for the elucidation of the migration speed of *Babesia* parasites in their vector tick, *Haemaphysalis longicornis*, has been developed using an artificial feeding system with quantitative PCR method. The detectable DNA of *Babesia* parasites gradually disappeared in the tick midgut at 1 day post engorgement (DPE), and in contrary increased in other organs. The results indicated that the *Babesia* parasite passed the *H. longicornis* midgut within 24 hours post engorgement, migrated to the hemolymph, and then proliferated in the organs except the midgut. This time point may be an important curfew for *Babesia* parasites to migrate in the tick lumen. We also visualized the *Babesia* parasites in the experimentally infected ticks and in their eggs using IFAT for detecting their cytoskeletal structure, which suggested the successful tick infection and transovarial transmission of the parasite. This model will shed light on the further understanding of tick-*Babesia* interactions.**

Ticks are notorious hematophagous ectoparasites of almost terrestrial vertebrates and well known as a unique vector of various deadly diseases, such as Lyme borreliosis, tularemia, anaplasmosis, babesiosis, theileriosis, tick-borne encephalitis, and severe fever with thrombocytopenia syndrome (SFTS)[1,2]. About 900 tick species, including approximately 700 ixodids and 200 argasids, are distributed throughout the world[3]. Recent analysis of the tick microbiome indicates that ticks harbor a wide variety of microorganisms[4]. Pathogens, including bacteria, protozoa, and viruses, are taken up with the blood meal and exposed to a potentially hostile environment in the tick's midgut before they invade the gut cells. It is assumed that the tick-pathogen interaction in relation to the adaptation and proliferation of the pathogens in ticks and their successful transmission to the vertebrate hosts is maintained by molecular mechanisms[5,6]. It has been shown that the bioactive molecules such as longicin and longipain from *H. longicornis* critically regulates the transmission of *Babesia* parasites in the tick[7,8].

Babesiosis is caused by intraerythrocytic apicomplexan parasites which belong to the genus *Babesia* and is mainly transmitted by tick vectors to a variety of vertebrate hosts, including wild and domestic animals and also humans[9,10]. *Babesia* species undergo a complex developmental cycle in the vertebrate host and tick, somewhat analogous to that of malaria parasites and their mosquito vector. With the worldwide distribution of ixodid ticks, babesiosis is the second most common blood-borne disease of mammals. The major tick vectors of

[1]Laboratory of Infectious Diseases, Joint Faculty of Veterinary Medicine, Kagoshima University, Korimoto, Kagoshima 890-0065, Japan. [2]Department of Pathological and Preventive Veterinary Science, The United Graduate School of Veterinary Science, Yamaguchi University, Yoshida, Yamaguchi 753-8515, Japan. [3]Department of Parasitology, Kitasato University School of Medicine, Kitasato, Minami, Sagamihara, Kanagawa 252-0374, Japan. [4]Department of Parasitology, Faculty of Veterinary Science, Bangladesh Agricultural University, Mymensingh-2202, Bangladesh. [5]National Institute of Animal Health, Kannondai, Tsukuba, Ibaraki 305-0856, Japan. [6]Laboratory of International Prevention of Epidemics, Graduate School of Life and Environmental Sciences, Osaka Prefecture University, Gakuen-cho, Nakaku, Sakai, Osaka 599-8531, Japan. [7]National Research Center for Protozoan Diseases, Obihiro University of Agriculture and Veterinary Medicine, Inada, Obihiro, Hokkaido 080-8555, Japan. Correspondence and requests for materials should be addressed to T.H. (email: htakeshi@med.kitasato-u.ac.jp) or T.T. (email: tetsuya@rms.kagoshima-u.ac.jp)

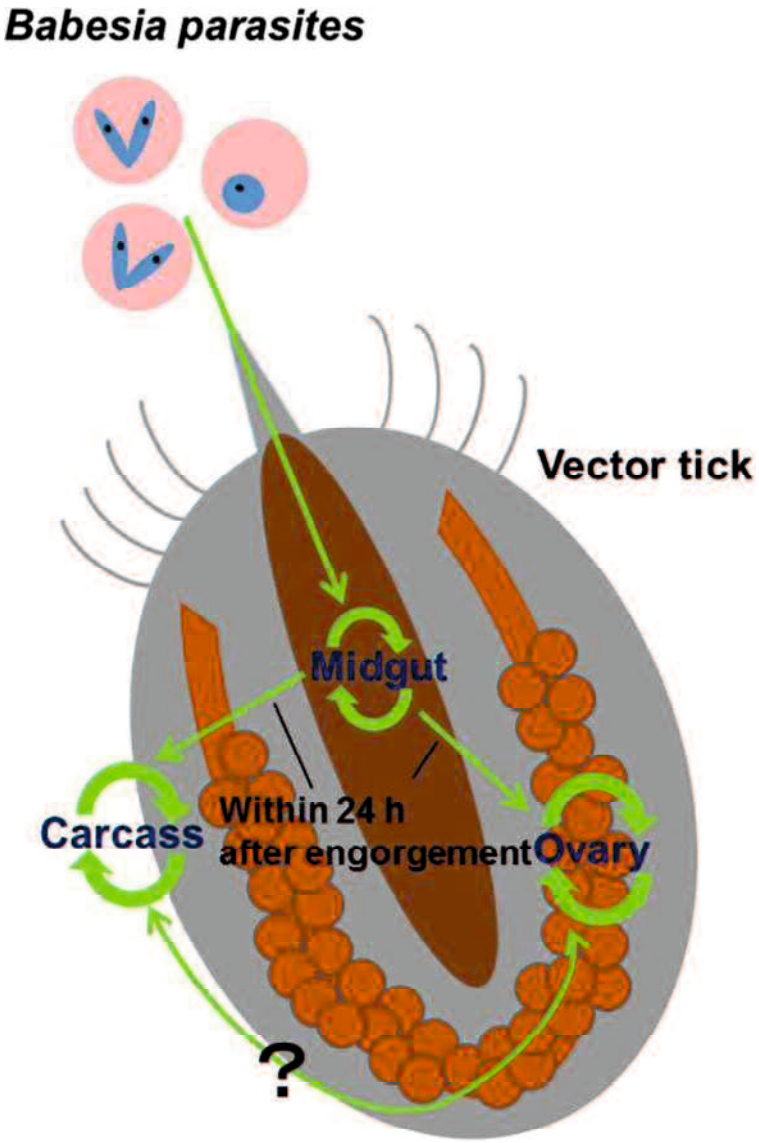


**Graphical abstract from:**

Maeda, H., Hatta, T., Alim, M.A., Tsubokawa, D., Mikami, F., Matsubayashi, M., Miyoshi, T., Umemiya-Shirafuji, R., Kawazu, S., Igarashi, I., Mochizuki, M., Tsuji, N., Tanaka, T. (2016). Establishment of a novel tick-*Babesia* experimental infection model. *Sci. Rep.*, ***6***, 37039.

Veterinary Parasitology 233 (2017) 39–42

Contents lists available at ScienceDirect

Veterinary Parasitology

journal homepage: www.elsevier.com/locate/vetpar

Short communication

# Initial development of *Babesia ovata* in the tick midgut

Hiroki Maeda[a,b], Takeshi Hatta[c,**], M. Abdul Alim[d], Daigo Tsubokawa[c], Fusako Mikami[c], Kodai Kusakisako[a,b], Makoto Matsubayashi[e], Rika Umemiya-Shirafuji[f], Naotoshi Tsuji[c], Tetsuya Tanaka[a,b,*]

[a] Laboratory of Infectious Diseases, Joint Faculty of Veterinary Medicine, Kagoshima University, Korimoto, 1-21-24 Korimoto, Kagoshima 890-0065, Japan
[b] Department of Pathological and Preventive Veterinary Science, The United Graduate School of Veterinary Science, Yamaguchi University, Yoshida, Yamaguchi 753-8515, Japan
[c] Department of Parasitology, Kitasato University School of Medicine, 1-15-1 Kitasato, Kitasato, Minami, Sagamihara, Kanagawa 252-0374, Japan
[d] Department of Parasitology, Faculty of Veterinary Science, Bangladesh Agricultural University, Mymensingh 2202, Bangladesh
[e] Laboratory of International Prevention of Epidemics, Graduate School of Life and Environmental Sciences, Osaka Prefecture University, Gakuen-cho, Nakaku, Sakai, Osaka 599-8531, Japan
[f] National Research Center for Protozoan Diseases, Obihiro University of Agriculture and Veterinary Medicine, Inada, Obihiro, Hokkaido 080-8555, Japan

ARTICLE INFO

*Article history:*
Received 13 October 2016
Received in revised form
23 November 2016
Accepted 26 November 2016

*Keywords:*
*Babesia ovata*
Midgut stage
Midgut contents
Artificial induction

ABSTRACT

The initial development of *Babesia ovata* in the midgut of the vector tick *Haemaphysalis longicornis* has been demonstrated through in vitro and in vivo studies. Although the research on the partial developmental cycles of *B. ovata* in the tick midgut was performed in our previous study by using ticks fed on experimentally *B. ovata*–infected cattle, detailed information on the developmental stages of *B. ovata* in *H. longicornis* was limited. This report describes the sequential development of stages of *B. ovata* in an in vitro study using *B. ovata*–infected erythrocytes and tick midgut contents. The in vivo study also confirmed the developmental stages in the midgut contents of artificially *B. ovata*–infected ticks. In this observation, we have recognized the distinct forms of *B. ovata* developmental stages in the tick midgut; the aggregation forms and ray bodies with shorter spikes and light-stained cytoplasm were shown by Giemsa staining. The similarities and differences of the stages as compared to previous reports have been discussed.



*Babesia* species are tick-borne apicomplexan protozoa that cause babesiosis and affect a wide range of wild and economically important domestic animals as well as humans. *Babesia* organisms show drastic morphological changes in tick tissue when they are transferred from the erythrocytic stages of vertebrate hosts (Chauvin et al., 2009; Florin-Christensen and Schnittger, 2009; Mehlhorn and Schein, 1984). Since the first discovery and detailed drawings of *Babesia* development in the tick midgut (Kleine, 1906; Koch, 1906), several studies on the midgut form of *Babesia* species have been reported (Gough et al., 1998; Higuchi et al., 1989b; Mehlhorn et al., 1980; Zapf and Schein, 1994). *Babesia ovata*, transmitted by the *Haemaphysalis longicornis* tick vector, is a less pathogenic cattle *Babesia* sp. compared to other virulent *Babesia* spp. such as *Babesia bovis* and *Babesia bigemina*. However, concomitant infection in cattle with *B. ovata* and *Theileria orientalis* is known to cause an induction of clinical anemia (Sivakumar et al., 2012). The *B. ovata* species has recently become a focus of clinical and molecular biological research. The transgenic *B. ovata* is also available as a tool for studying the tick stage of *Babesia* (Hakimi et al., 2016). Higuchi et al. worked extensively on the development of *B. ovata* in *H. longicornis* ticks dropped from experimentally *B. ovata*–infected cattle. They reported the development of *B. ovata* in the midgut, salivary glands, and hemolymph of the nymphal tick and also in the ovary and eggs of the adult (Higuchi et al., 1987, 1989a, 1989b, 1991, 1994). However, study on the tick stage of *B. ovata* in the adult tick has not progressed, and our knowledge of the entire lifecycle of *B. ovata* from morphological study is insufficient. In this report, we have focused on the initial developmental stages of *B. ovata* in the adult tick midgut by a comparative study from the in vitro culture system and in vivo study using an artificial feeding system for *H. longicornis* (Hatta et al., 2012).

*B. ovata* (Miyake strain) and *H. longicornis* (Okayama strain) maintained at the Department of Parasitology, Kitasato Univer-

* Corresponding author at: Laboratory of Infectious Diseases, Joint Faculty of Veterinary Medicine, Kagoshima University, 1-21-24 Korimoto, 890-0065, Kagoshima, Japan.
** Corresponding author.
*E-mail addresses:* htakeshi@med.kitasato-u.ac.jp (T. Hatta), k6199431@kadai.jp (T. Tanaka).

http://dx.doi.org/10.1016/j.vetpar.2016.11.020
0304-4017/

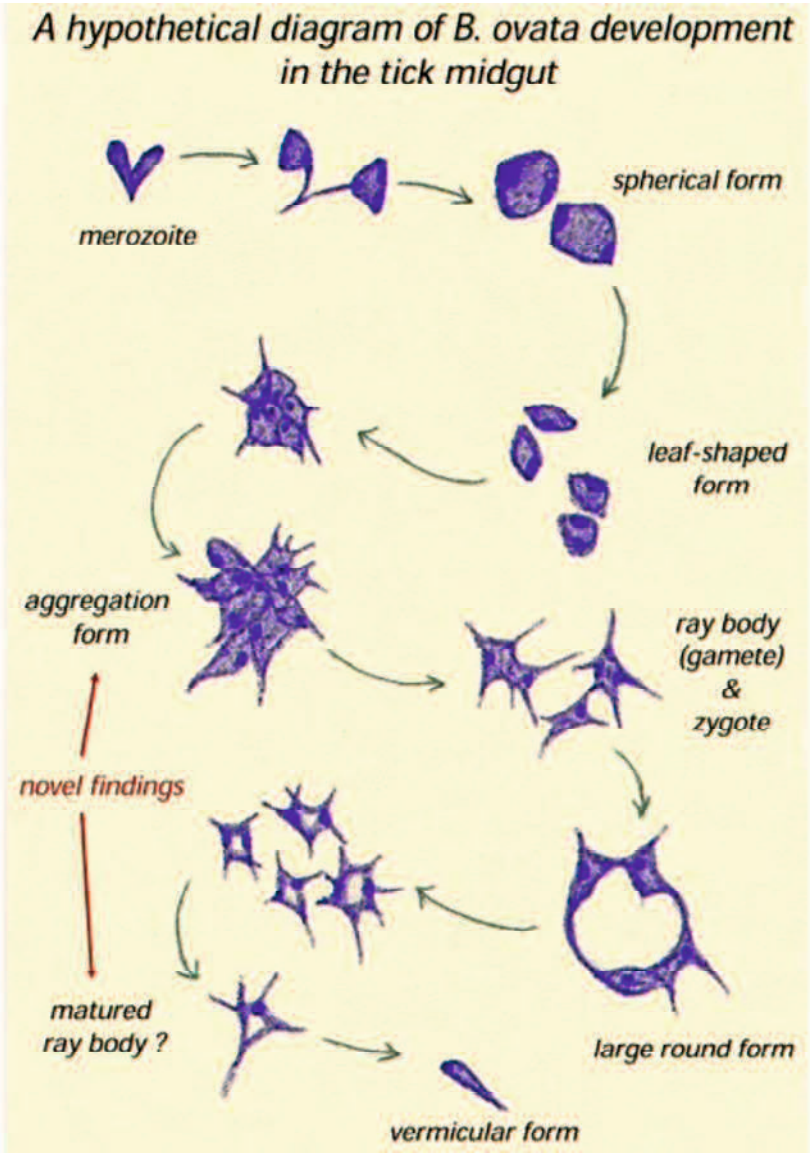


**Graphical abstract from:**

Maeda, H., Hatta, T., Alim, M.A., Tsubokawa, D., Mikami, F., Matsubayashi, M., Umemiya-Shirafuji, R., Tsuji, N., Tanaka, T. (2017). Initial development of *Babesia ovata* in the tick midgut, *Vet. Parasitol.*, ***233*****,** 39-42.